TR-179

TECHNICAL REPORT

ON THE GENERATION AND DIRECTIONAL RECORDING OF WAVES IN THE ARCTIC OCEAN

LEONARD A. LESCHACK

Formulation Branch

Oceanographic Prediction Division

SEPTEMBER 1965

U. S. NAVAL OCEANOGRAPHIC OFFICE
WASHINGTON, D. C. 20390
Price 90 cents

ABSTRACT

An experiment to investigate the directional nature and the possible generation mechanisms for waves on the Arctic Ocean, an ocean almost entirely covered with sea ice, is described. The waves under consideration have periods between 10 and 100 seconds and amplitudes between 0.001 and 2.0 centimeters. These waves have been previously observed with gravimeters and seismographs and have been described in the literature.

In the present work an array of two continuously recording gravimeters 1,240m apart was established at drift station ARLIS II. The records obtained were examined by cross-spectrum analysis techniques. Observed waves with distinct periods were associated with a storm over Siberia.

A continuously recording microbarograph sensitive to atmospheric micropressure oscillations in the 10- to 100-second period range was also installed at ARLIS II. Distinct oscillations were observed in this period range having amplitudes of from 20 to 400 dynes/cm^2. Power spectra of micropressure records made before, during, and after a storm show that the oscillation amplitude is proportional to the period of the oscillation and speed of local winds. Cross-correlation between the micropressure records and wave records taken with a gravimeter at the same location as the microbarograph shows a positive correlation between the micropressure waves and the ocean waves. This correlation appears to vary with the direction of the local surface wind and may be related to the orientation of pressure ridges in the ice pack. Although the nature of the micropressure oscillations could not be determined with only the one sensor used, the oscillations were assumed to be progressive waves. These waves contained sufficient force to bend the ice and generate the observed water waves.

FOREWORD

The U.S. Naval Oceanographic Office has been engaged in exploratory development of methods of sea ice observation and prediction of sea ice processes which affect arctic military operations and warfare since 1960. A thorough understanding of periodicity and other oscillatory properties of sea ice is extremely important for ultimate prediction of ice deformation processes. Since deformation processes determine the origin, development, and decay of open water and ridging features throughout the 2 to 4 million square miles of ice-covered Arctic Basin, they profoundly affect global heat balance and quantity of ice produced during any given season.

This report presents the research results of an initial attempt to employ gravimeters for investigation of longwaves on the Arctic Ocean and ascribes generation mechanisms to these waves. The evidences relating vertical ice oscillations to atmospheric micropressure records suggest that this approach be continued.

Comments and criticisms concerning the experimental design or interpretation of the results are welcome and should be addressed to the Commander, U.S. Naval Oceanographic Office.

DENYS W. KNOLL
Rear Admiral, U.S. Navy
Commander
U.S. Naval Oceanographic Office

TABLE OF CONTENTS

		Page
1.	INTRODUCTION	1
	a. Preliminary Remarks and Review of Literature	1
	b. Purpose and Design of Experiment	3
2.	INSTRUMENTATION	5
	a. Site	5
	b. LaCoste-Romberg Gravimeter #22	6
	c. World-Wide Gravimeter #5	6
	d. Microbarograph	7
	e. The Records	8
3.	DATA REDUCTION	8
	a. Design Considerations	8
	b. Power Spectra and Cross Spectra	15
	c. Corrections to the Data	16
	d. Length of Time Series	17
4.	THE 2-ELEMENT ARRAY	17
	a. General Description	17
	b. Direction Finding	21
	c. Beam Width	25
	d. Evaluation of the Results of the 2-Element Array	26
5.	SIMULTANEOUS WAVE AND PRESSURE SPECTRA BEFORE, DURING, AND AFTER A STORM	26
	a. Introduction	26
	b. Microbarograph Records	26
	c. Gravimeter Records	30
6.	DISCUSSION	33
	a. The Relationship of Atmospheric Micropressure Fluctuations to Water Waves	33
	b. Energy Transfer Considerations	36
7.	CONCLUSIONS AND RECOMMENDATIONS FOR FURTHER WORK	39
	ACKNOWLEDGEMENTS	41
	REFERENCES	43

1. INTRODUCTION

a. Preliminary Remarks and Review of Literature

The study of the origin and behavior of wave motion on the open ocean has received considerable attention during the past decade. The primary impetus for this work has been provided by the U.S. Navy. The Navy has a continuing interest in being able to predict routinely the sea state at a given location on the ocean, much the same as the Weather Bureau predicts the weather. The greater part of the Navy's work has been oriented toward the ice-free, non-polar areas, with little or no attention being given to the nature of ocean waves in extensive areas of ice-covered oceans.

Wave motion and wave generation do not cease in polar oceanic areas because a layer of ice has been placed on the water surface, although one would intuitively expect severe attenuation of wave amplitudes. This attenuation has been repeatedly reported by mariners navigating in such waters and is one of the most outstanding features observed when sailing from the open ocean into water with numerous ice floes.

It was not until Robin's studies with a shipborne wave recorder in the Weddell Sea were completed (1963) that any quantitative measure of the attenuation of wave motion due to ice cover became available. Robin showed that: (1) the ice cover, usually floes 1 to 3 meters thick, could be considered elastic plates for the frequencies and amplitudes encountered in the ice pack, (2) the waves observed in the ice field had ample energy to bend the floes and still propagate, and (3) the wave energy penetrating the pack was proportional to λ^4 / h^3 where λ = wavelength, and h = ice thickness.

The vertical component of wave motion deep within the ice pack had been observed with gravimeters prior to Robin's study, although quantitative discussions of the wave-producing mechanism have been attempted only recently. Crary et al. (1952) made gravity observations as part of a geophysical program on the pack ice of the Beaufort Sea in 1951. They reported that the optical crosshair of the gravimeter oscillated about the instrument's null-position, usually within the range of the scale stops, with periods between 20 and 40 seconds. It was therefore necessary to average a series of values taken over an interval of several cycles to obtain a representative value for the gravity field at a given location. Further gravity observations were made by Crary and Goldstein (1959) on Arctic Drift Station T-3 between 1952 and 1954. As part of the geophysical program, they routinely made daily gravity measurements, reading the gravimeter every 5 seconds for an interval of 5 to 6 minutes. A statistical study of these oscillations showed periods ranging from 23 to 61 seconds with 70 percent of occurrences falling between 33 and 43 seconds. They found no correlation between oscillation amplitudes and periods with either atmospheric pressure or surface wind speeds. They did, however, observe a seasonal trend. The overall amplitude showed peaks during March and November with a low in July. July, although having the least amplitude, has the maximum occurrences of long-period energy. Hunkins (1962) made

a comprehensive study of waves on the Arctic Ocean, using a seismograph, tide gage, and gravimeter to examine the spectrum of waves with periods between 10^{-1} and 10^{5} seconds. In particular, he observed (1) a phase difference in simultaneous records of two gravimeters read 400m apart and (2) correlated surface wind speed with the maximum amplitudes of the oscillations recorded by both a seismograph and a gravimeter. Thus, he showed that these oscillations were progressive waves and, by Fourier analyses, computed apparent phase velocities of several of the components. By correlating surface wind speed with maximum oscillation amplitude, he found that when the wind exceeded 20 to 24 knots there was a significant positive correlation; below this speed there was no correlation. He therefore suggested 20 to 24 knots as the threshold excitation value.

LeSchack and Haubrich (1964), using power spectrum techniques, examined the characteristics of several long gravity records taken in the Arctic. They showed the similarity between the spectra of two records taken simultaneously at sites more than 1km apart. Representative values for ice displacement as a function of wave period were given.

Sytinskiy and Tripol'nikov (1964) discussed the observations of waves measured with a tripartite array of earthquake seismographs at their stations N-13 and N-14. They observed progressive waves having the same period range as previously reported and amplitudes averaging 0.02 to 0.025cm, with maximum peaks of 0.1cm in deep water. Maximum amplitude on the continental shelf was 0.3cm. These amplitude values were consistent with those computed by LeSchack and Haubrich.

Sytinskiy and Tripol'nikov attempted to measure phase velocities and wave directions by comparing the records from the tripartite array, presumably by matching peaks of the same phase. The phase velocity values were rather scattered but fell mainly between 20 and 60 m/sec. They attributed the velocity scatter to wave interference at the point of observation. They noted, as Hunkins had, the general positive correlation of wave amplitudes with high local surface wind speed. Accordingly, they examined a wave record made during a sudden gust of wind and reported the following sequence:

(1) A short burst of energy of about 3-second period due to "bobbing" of the ice computed from equation (1).

$$T = 2\pi(\rho h/\rho' g)^{1/2} \qquad (1)$$

where T = period (sec)
ρ = ice density
h = ice thickness
ρ' = water density
g = gravity

(2) This "bobbing" was superimposed on a 12- to 15-second wave that seemed to be initiated by the wind gust and continued for several minutes thereafter. They believed that the generation of the 12- to 15-second wave was analogous to oscillations that would theoretically be produced by a load

moving across an infinite, elastic plate floating on an ideal liquid. For ice over deep water, they used the following expression:

$$T_o = 2\pi \left[\frac{\gamma h g^3}{D}\right]^{-1/6} \qquad (2)$$

where T_o = natural period (sec)
γ = specific weight of ice (0.9 tons/m3)*
h = thickness of ice (3m)
g = gravity (9.83 m/sec2)

$$D = \frac{E h^3}{12(1-\mu^2)}$$

E = Young's modulus for ice (3 x 10^5 tons/m^2)*
μ = Poisson's ratio (0.35)

Using the above constants they obtained a value of T_o = 16 sec. Taking into account the depth of water at the observation point (150 to 200m) they arrived at a value, T_o = 12 sec. According to their theory, a vertical load moving over an infinite, elastic plate floating on an ideal liquid will generate not only waves of period T_o but will also produce "free" oscillations or swell with period T_w where $T_o \leq T_w < \infty$. The oscillations of period T_o are attenuated by cylindrical spreading, while those of T_w are primarily attenuated in proportion to time. The waves with period T_w, therefore, may propagate over considerably greater distances than those of period T_o. Their observations were in agreement with those predicted in theory; however, considerably more observations would be necessary to rule out other modes of wave generation.

b. Purpose and Design of Experiment

It clearly appears that oscillations recorded with seismographs and gravimeters, as described in the literature, are vertical components of ordinary gravity waves. Furthermore, correlation between wind speed and wave amplitude exists but only above some threshold value. It is therefore interesting to study more fully the nature of these waves, their directionality and mode of propagation, and the causes of their generation. For example, are they associated with storm centers as are waves on the open ocean, and is the moving load mechanism suggested by Sytinskiy and Tripol'nikov the primary energy source?

To answer these questions, a series of measurements of these waves was begun in June 1961 from drift station ARLIS II in the Arctic Ocean. A LaCoste-Romberg undersea gravimeter, modified to record the vertical motion of ice automatically on strip charts, was installed on the drift station. Nearly continuous recordings of wave acceleration were made during the summer of 1961. Simultaneously, a microbarograph sensitive to micropressure variations between 6-second and 6-minute periods was placed in operation at the same location. Its output was also recorded on strip charts. In this manner,

*The units of Sytinskiy and Tripol'nikov

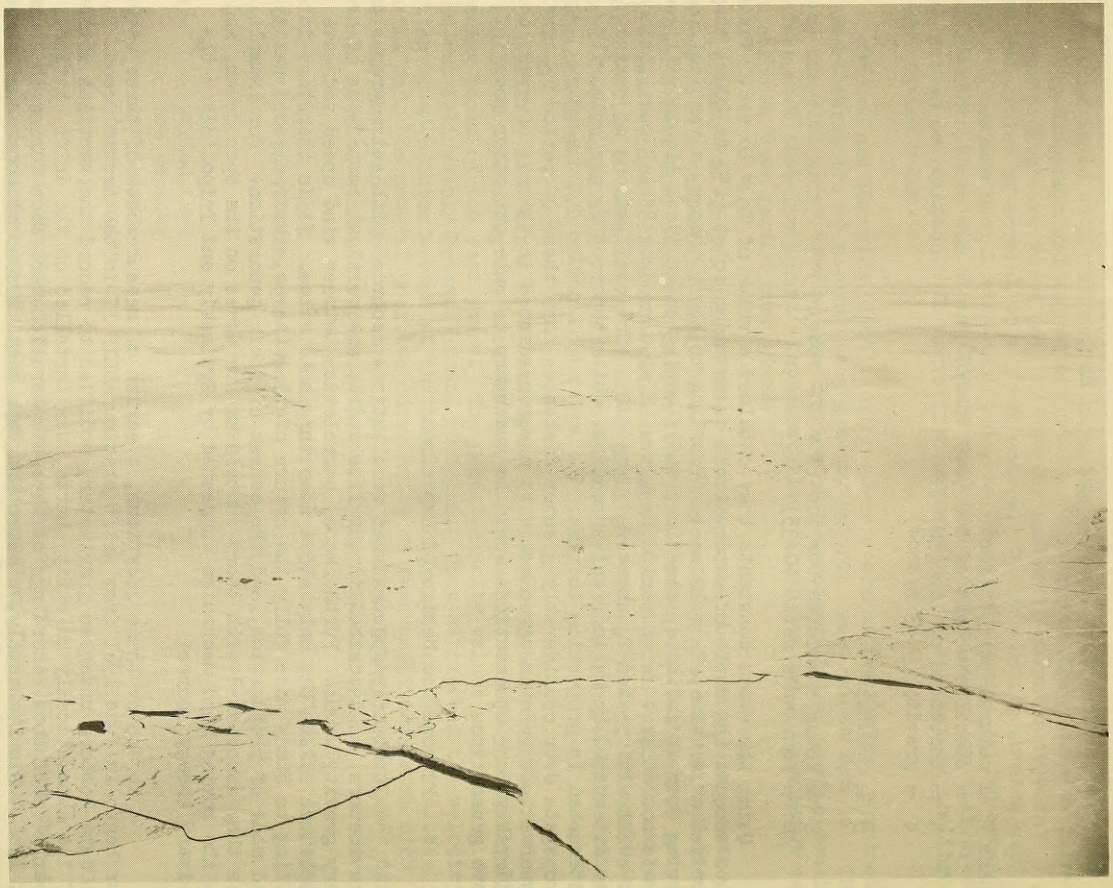

FIGURE 1 Ice Island ARLIS II, May 1961

the author hoped to correlate periodic pressure variations, if any, in the period range 10 to 100 seconds with the observed wave motion. In addition, a second gravimeter, a portable model, was located 1,240m from the primary gravimeter, so that a study of phase relationships of the waves could be made. Although the meters were operated simultaneously in this way for only a short interval, it was felt that much insight into the nature of these waves could be gained from the data.

2. INSTRUMENTATION

a. Site

All wave measurements were made at ARLIS II (figure 1), an arctic drift station operated by the Office of Naval Research's Arctic Research Laboratory at Barrow, Alaska. ARLIS II is a block of glacial ice which originated from an Ellesmere Ice Shelf and became entrapped in the constantly moving pack ice of the Arctic Ocean Basin (LeSchack, 1961). At the time of these observations, its dimensions were 3km by 6.5km by about 20m in thickness. The station, drifting slowly westward during early summer, moved from a distance of 110 miles from Point Barrow to a distance of 180 miles during the course of the observations. Water depth beneath the station varied from 150 to 1,600m along the station's track (figure 2).

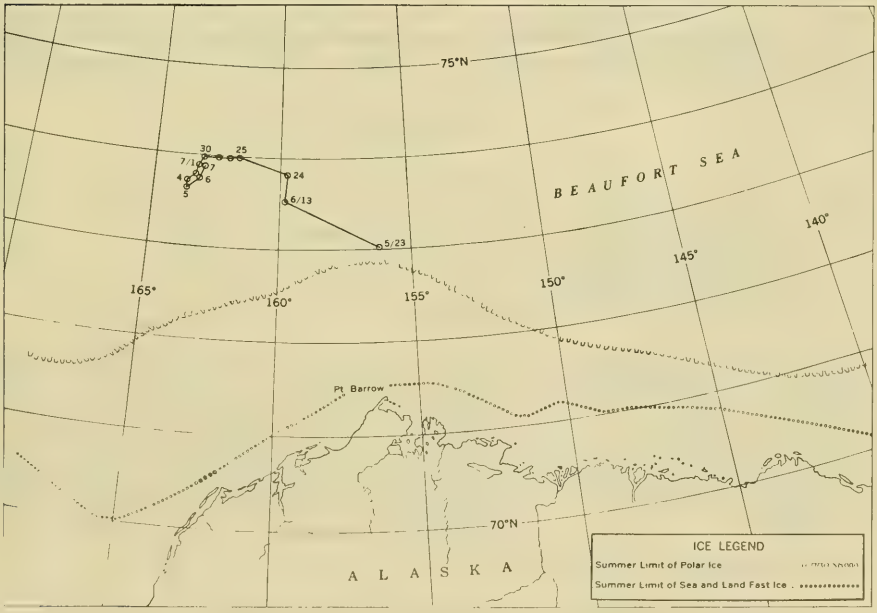

FIGURE 2 Track of ARLIS II, May—July, 1961

The gravimeter and microbarograph were installed in a heated building at the campsite located 650m from the edge of the island. The second gravimeter was set up in the center of an adjacent ice floe separated from the island by two pressure ridges. On 3 June 1961 the two gravimeters were read simultaneously.

b. LaCoste-Romberg Gravimeter #22

This instrument was originally built for underwater gravity measurements, thus, provision for reading it remotely had already been incorporated in the gravimeter's construction. It was, therefore, relatively simple to modify the meter so that its output could be recorded on Esterline-Angus strip charts. This was desirable for long automatic recordings of wave records — an impossibility with the usual method of visual recording.

The gravimeter was mounted on a pedestal that passed through a hole in the floor of the building. The pedestal was frozen solidly into the ice and was not in contact with the building.

The sensitivity of the gravimeter could be adjusted between limits sufficiently wide to keep large amplitude peaks on scale, while intervals of low amplitude could easily be read. Sensitivity was varied by adjusting the longitudinal level of the gravimeter. Sensitivity calibrations for all values of leveling were made on solid land at Point Barrow, Alaska, prior to operation on the ice.

Varying the sensitivity to match wave conditions caused a variation of the instrument's natural period and damping constant according to the following equations:

$$h = (K)^{1/2} d \qquad (3)$$

$$T = (K)^{1/2} T_0 \qquad (4)$$

where h = actual damping
K = sensitivity in eyepiece divisions per dial division
d = critical damping
T = natural period (sec)
T_0 = 22.4 sec (instrument constant)

For the two sensitivities used in this work, the natural periods and damping constants were $T = 26.4$ sec, $h = 1.18$ critical, and $T = 18.6$ sec, $h = 0.83$ critical. Since both damping constants were greater than 0.707 critical, the problem of resonance was not encountered (Richter, 1958). The response, however, fell off 6db per octave below the instrument's natural period, resulting in recording little energy with periods less than 10 seconds. The problem of aliasing, therefore, was avoided since the period range of interest was 10 to 100 seconds.

c. World-Wide Gravimeter #5

This is a portable gravimeter used on the pack ice as the second element of a 2-element array. The wave motion was read visually and recorded every 5

seconds for 90 minutes on the one occasion when the 2-element array was used. The instrument had a natural period of 7 seconds and was critically damped. Although this gravimeter was inherently more sensitive to shorter periods than was the LaCoste-Romberg #22, there did not appear to be any energy with periods less than 10 seconds.

A general discussion of the physical construction and theory of gravimeters can be found in any text on exploration geophysics, for example, Nettleton (1940).

d. Microbarograph

Recordings of micropressure variations in the period range 10 to 100 seconds were desired for correlation with observed ocean waves. A T-21 microbarograph using pressure transducer #7156 and amplifier #14779 was used to automatically record the vertical micropressure variations. This instrument was built by the U.S. Navy Electronics Laboratory for the Air Force Cambridge Research Center.

The transducer is basically a condenser microphone composed of two enclosed volumes separated by a thin aluminum diaphragm. The condenser is formed by the diaphragm and a backing plate with 0.005-inch separation. Each enclosed volume is vented to the atmosphere, but the time constant of each is different. Thus, for a given rate of atmospheric pressure change, a pressure difference exists across the diaphragm. Frequency response of the transducer is determined by choice of acoustic vents in the enclosed volumes. The response curve for the instrument used in this work is shown in figure 3.

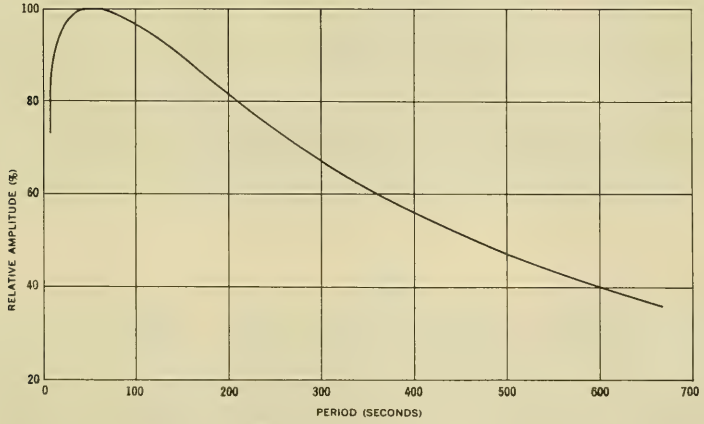

FIGURE 3 Microbarograph Response Curve

The transducer was well insulated so that thermal variations, which would cause changes in pressure within the two enclosed volumes, would have a period considerably greater than the instrument's passband. The input of the microbarograph was simply a tube passing from the transducer through the wall of the building to the open air.

e. The Records

The outputs of the LaCoste-Romberg gravimeter and the microbarograph were recorded continuously on Esterline-Angus strip charts generally operated at a speed of three-fourths of an inch per minute. The output of the gravimeter was expressed in milligals (1 milligal = 10^{-3} cm/sec^2) as a function of time, and full-scale deflection was adjusted to either 28 or 35 milligals.

The gravimeter records vertical acceleration of the ice as a function of time; a seismograph records displacement directly. Displacement of the wave with respect to time is most often observed in wave studies. Gravimeters have been used in this work because of their portability and ease of operation on ice in comparison to seismographs. In the analysis of these records the frequency characteristics of the narrow-band energy peaks will be essentially the same whether displacement or acceleration is recorded for the period range being considered. A conversion is necessary, however, when spectral power density in terms of displacement is desired. This is accomplished by dividing the acceleration spectrum by the fourth power of the angular frequency (ω^4).

If the ice were not in motion the output of the gravimeter would be a straight line in the center of the chart, representing a constant downward acceleration of gravity with time. Oscillation above or below this line represents a positive or negative change, respectively, of the downward acceleration at a given instant about the constant gravity value at that point in space. Positive peaks on the strip chart, therefore, correspond to positive displacements of the ice.

The output of the microbarograph is recorded in units of dynes/cm^2. Full-scale deflections of 270 and 500 dynes/cm^2 were used in this work with pressure increasing in the positive y direction.

Samples of simultaneous pressure and wave records for 5 and 6 July 1961 are shown in figures 4a, b, and c.

3. DATA REDUCTION

a. Design Considerations

Power spectrum analysis (Blackman and Tukey, 1958) and cross-spectrum techniques discussed by Munk et al. (1959) are probably the most powerful tools available for analyzing statistical properties of wave motion with a stationary gaussian distribution. The gravity waves and micropressure fluctuations under consideration fall in this category. These techniques rely on data processing by high-speed digital computers. The data collection was undertaken with these processing techniques in mind.

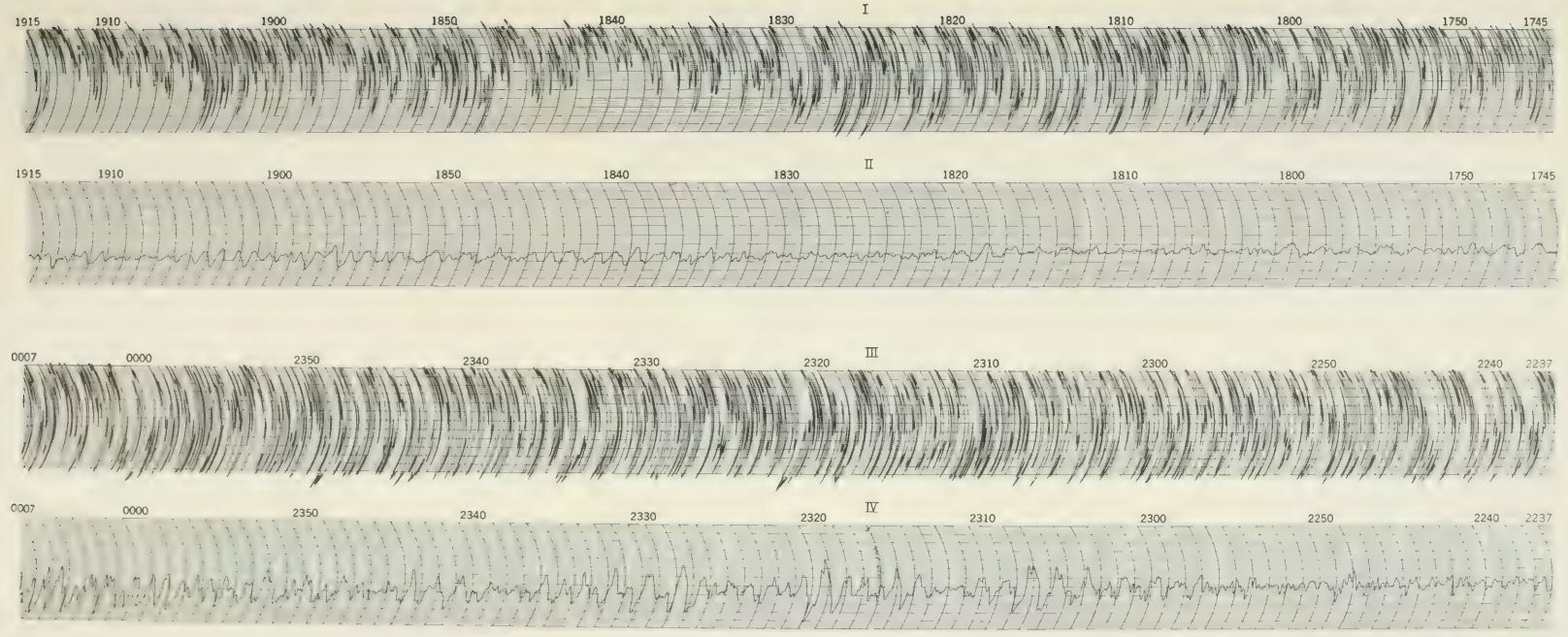

FIGURE 4a Simultaneous microbarograph and gravimeter records 5 July 1961 Microbarograph records are I and III, full-scale deflection, 270 dynes/cm^2 Gravimeter records are II and IV, full-scale deflection, 35 mgals

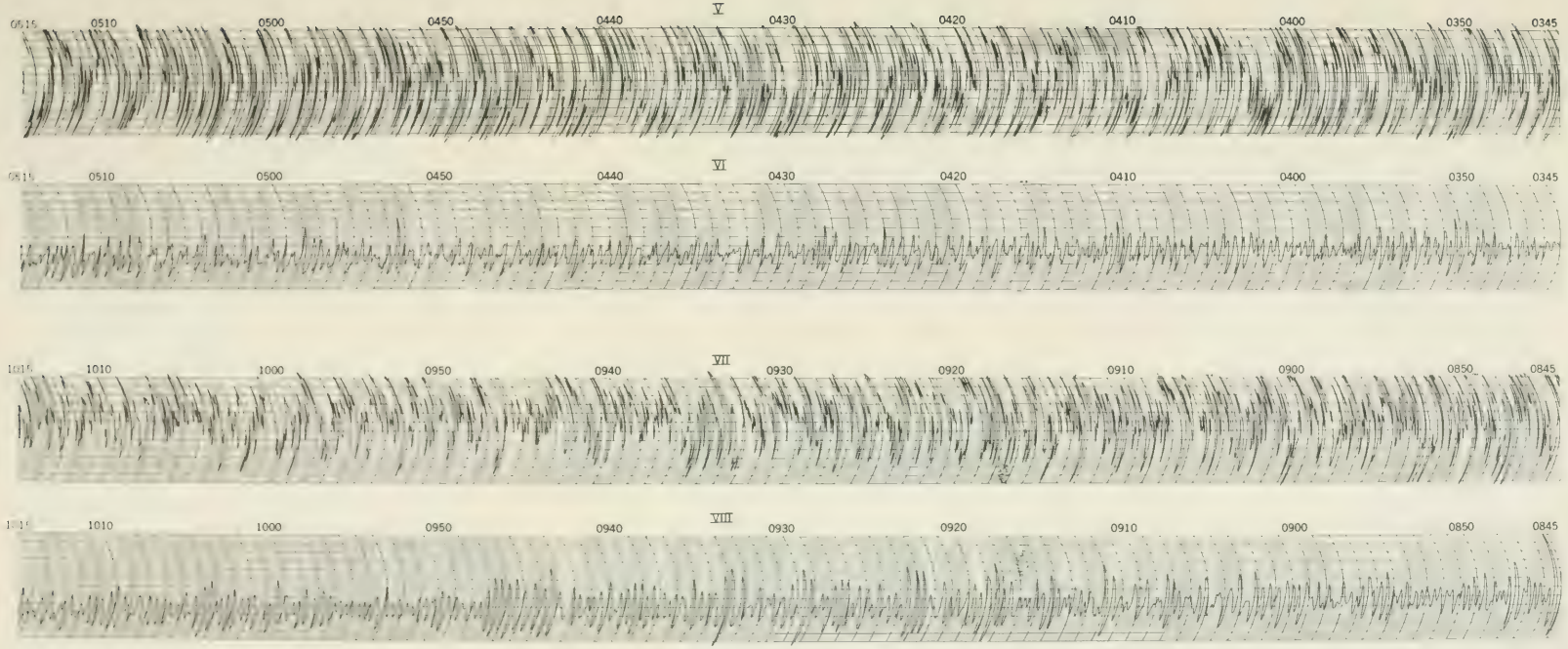

FIGURE 4b Simultaneous microbarograph and gravimeter records 6 July 1961. Microbarograph records are V and VII; full-scale deflection, 500 dynes/cm^2. Gravimeter records are VI and VIII; full scale deflection, 35 mgals

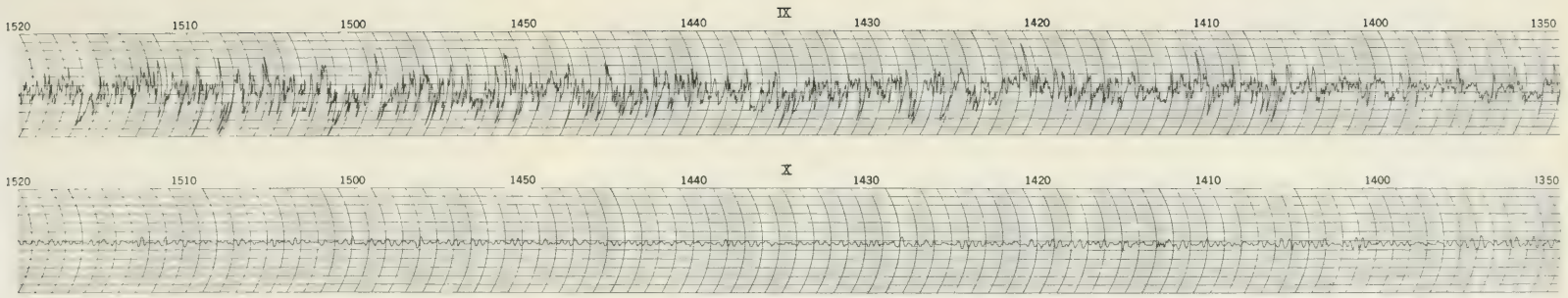

FIGURE 4c Simultaneous microbarograph and gravimeter records 6 July 1961. Microbarograph record is IX, full-scale deflection, 500 dynes/cm^2. Gravimeter record is X, full scale deflection 35 mgals.

It was necessary to digitize the analog records for computer processing. A sampling interval, ΔT, of 5 seconds was chosen to permit resolution of energy at spectral periods as low as 10 seconds ($(2\Delta T)^{-1}$ = the Nyquist frequency) and to avoid aliasing. Since the gravimeter records showed little energy with periods less than 10 seconds, aliasing was no problem. However, there was some short-period, but low amplitude, energy visible on the microbarograph records. It was not considered appreciable; hence a sampling interval of 5 seconds was used to produce both time series.

Power spectrum and cross-spectral analyses were then computed directly from these time series. No low frequency filtering was applied to the data, because drift and tidal effects, although observable, had less amplitude than the measured waves. This long-period energy is assigned to the first few lags of the spectrum. Therefore, with the number of lags used in the following analyses (100, 50, and 20), the best spectral estimates are found for periods of 100 or less seconds.

b. Power Spectra and Cross-Spectra

Given two time series $\eta_r(t)$ and $\eta_s(t)$, their time average

$$\rho_{rs}(\tau) = \overline{\eta_r(t)\,\eta_s(t+\tau)} \tag{5}$$

is called covariance of the two series.

The quantities

$$C_{rs}(f) = \int_{-\infty}^{\infty} \rho_{rs}(\tau) \cos 2\pi f\tau \, d\tau \tag{6}$$

and

$$Q_{rs}(f) = \int_{-\infty}^{\infty} \rho_{rs}(\tau) \sin 2\pi f\tau \, d\tau \tag{7}$$

are the co- and quadrature spectra, respectively. For the special case when r = s, Qrr(f) = 0, and Crr(f) is called the power spectrum. The quantity Crr(f) has been used in this work for computing spectral estimates of single time series.

When a pair of time series was compared for coherence, as in the case of simultaneous micropressure and gravity records or simultaneous gravity records from two different locations, the following relationships were used:

$$R_{rs}(f) = \left[\frac{C_{rs}^{\,2} + Q_{rs}^{\,2}}{C_{rr}\, C_{ss}} \right]^{1/2} \tag{8}$$

and

$$\phi_{rs}(f) = \tan^{-1}\left[\frac{Q_{rs}}{C_{rs}} \right] \tag{9}$$

where $R_{rs}(f)$ is the coherence between time series r and s, and $\phi_{rs}(f)$ is the phase of $\eta_s(t)$ minus the phase of $\eta_r(t)$ at frequency f. Thus if $\eta_s(t) = A \cos 2\pi ft$ and $\eta_r(t) = B \sin 2\pi ft$, the coherence $R_{rs}(f) = 1$ and the phase angle $\phi_{rs}(f) = 90^o$.

Although the maximum value of $R_{rs}(f) = 1$, this value would not be anticipated in nature. Instead, a lower value than one is usually obtained. According to Munk et al. (1959), the value above zero at which $R_{rs}(f)$ becomes meaningful can be expressed by:

$$95\% \text{ confidence limits of } \left[R_{rs}(f)\right]^2 = \frac{4}{DF}^* \qquad (10)$$

where DF = degrees of freedom = $(N - \frac{M}{4}) \Big/ \frac{M}{2}$

N = number of observations
M = number of lags

c. Corrections to the Data

Coherences computed from equation (8) are a function of only the frequency of the measured waves and are not dependent upon the relative change of signal amplitude at a given frequency, owing to the constant frequency response factor of each instrument. Also, the phase angle is not dependent upon this factor but only upon the frequencies and, of course, the phase difference between the frequencies. Thus, it has not been necessary to apply any correction to the data for those instrument response characteristics that affec only the amplitude of the recorded signal. Each instrument produces a phase shift of the recorded signal as a function of frequency. This delay is different for the two gravimeters used and must be considered when studying the phase relationships between two incoming signals.

The phase shift due to each instrument was calculated according to equation (11) (Richter, 1958)

$$\tan b = \frac{2h\tau T}{\tau^2 - T^2} \qquad (11)$$

where b = the phase shift in radians
h = the damping constant
τ = the natural period of the instrument (sec)
T = the wave period (sec)

The relative phase shift between the gravimeters was also computed. This value was then subtracted from the phase lag computed by the cross-correlation program.

---

*Equation (10) is an approximation derived from a complicated equation given in Munk et al. (1959). Since the writing of this paper, it has been learned from Dr. R. A. Haubrich, a colleague of Prof. Munk, that a better approximation is now in use: 95% confidence limits of $\left[R_{rs}(f)\right]^2 = 6/DF$. This increases the 95% confidence limit from 0.44 to 0.53. Examination of figures 8b, 9b, and 22, where this confidence limit is used, shows that the majority of those coherence peaks previously considered significant are still significant, and the conclusions based on these values still appear to be valid.

When wave spectra derived from both gravimeters are plotted on the same set of coordinates for direct comparison, corrections for instrument response must be applied. This was done by computing the $(\text{acceleration})^2$ response of each instrument and then applying this directly to the spectra plots. A similar correction derived from the microbarograph response curve (figure 3), although small, was applied to the micropressure spectra.

d. Length of Time Series

The number of 5-second observations used for the spectral analysis of each time series was a compromise between the best spectral estimate possible and the length of time that the power spectrum remained stationary. As mentioned above, the greater the number of observations for a given number of lags, the greater the number of degrees of freedom or the closer the estimated power spectrum is to the true but unknown spectral density. Examination of individual records and their power spectra show that for intervals greater than 45 to 60 minutes the spectra vary somewhat with slight shifts of peak energy with time. This can be seen when any of the 90-minute wave or micropressure records are divided into two 45-minute sections. Spectra for the two consecutive 45-minute time series of each record are compared in figures 5 and 6.

A 45-minute record appears to be optimum for obtaining stationarity and sufficient data points for a meaningful analysis. This was tested by dividing a typical 90-minute record into four equal, consecutive time series. Comparison of the frequency distribution of observed displacements for each adjacent series shows a good degree of stationarity from one series to another. Thus, 45-minute series have been used when the spectral distribution is more important than the overall estimate of spectral energy. For the latter, 90-minute records are used; this essentially doubles the number of degrees of freedom.

4. THE 2-ELEMENT ARRAY

a. General Description

The LaCoste-Romberg gravimeter #22 was installed at the ARLIS II campsite, and automatic recording began on 31 May 1961. On 3 June 1961 the World-Wide gravimeter #5 was set up on an ice floe adjacent to the ice island. This station was located 1,240m from the campsite on an azimuth of 143°T. The World-Wide gravimeter was read visually every 5 seconds for 90 minutes beginning 0215Z. A portion of these two records is shown in figure 7. An attempt was made to match amplitude peaks of the same phase. Although the choice was quite tentative, it suggested that a given phase arrived at the ARLIS II station 30 to 35 seconds before it did at the pack ice station. This would indicate an apparent average phase velocity of 33 meters per second.

The 90-minute record taken with this array was divided in two, and the spectra of each half were computed (figures 8a and 9a). The coherences and phase angles of the two sets of records were computed as described above and

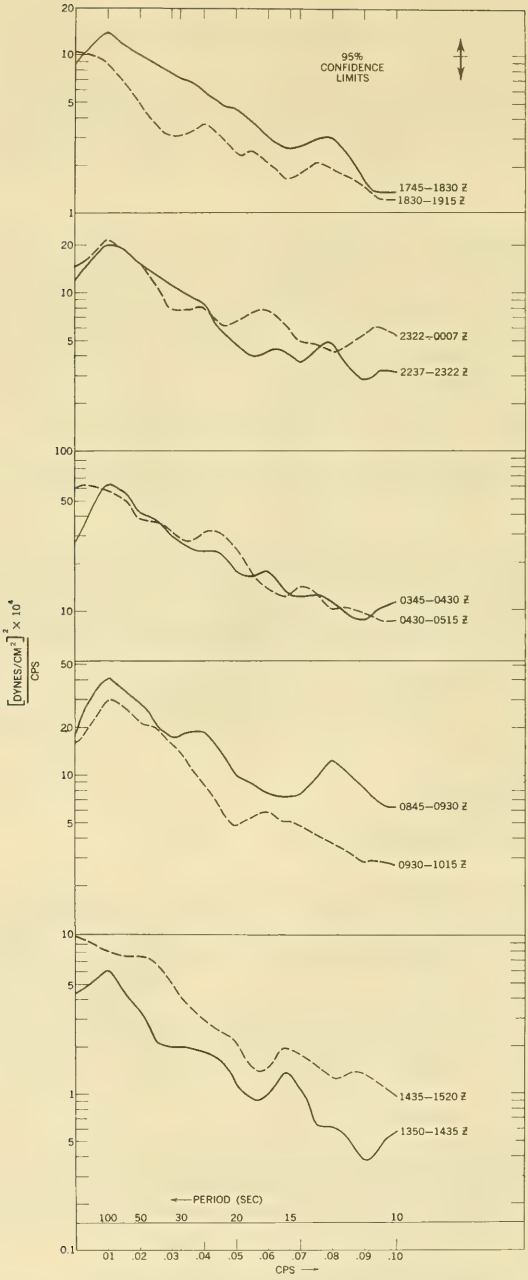

FIGURE 5 Power spectra of micropressure wave records taken during 5 and 6 July 1961. Spectra are computed separately for each half of the 90-minute records. Spectra are not corrected for instrument response.

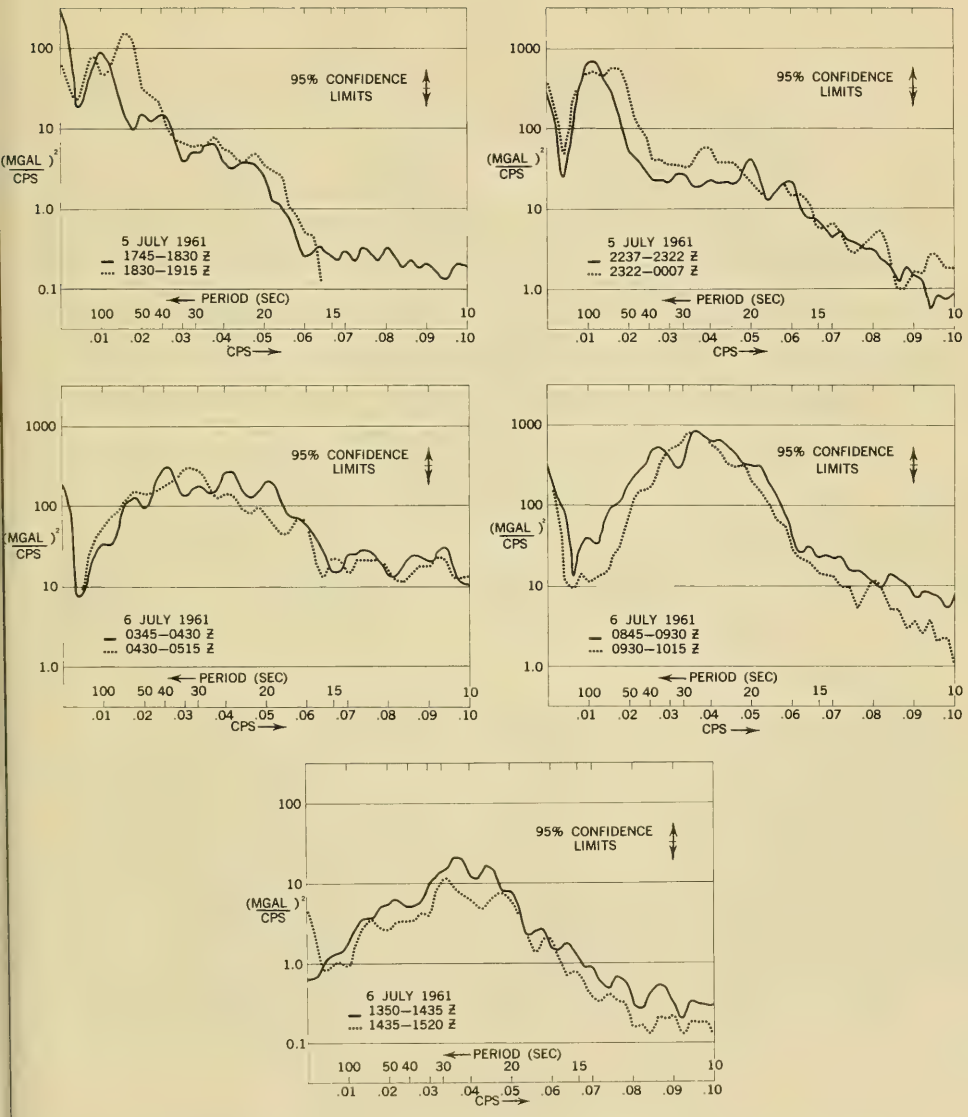

FIGURE 6 Power spectra of 5 water wave records taken during 5 and 6 July 1961—Spectra are computed separately for each half of the 90-minute records. Spectra are not corrected for instrument response.

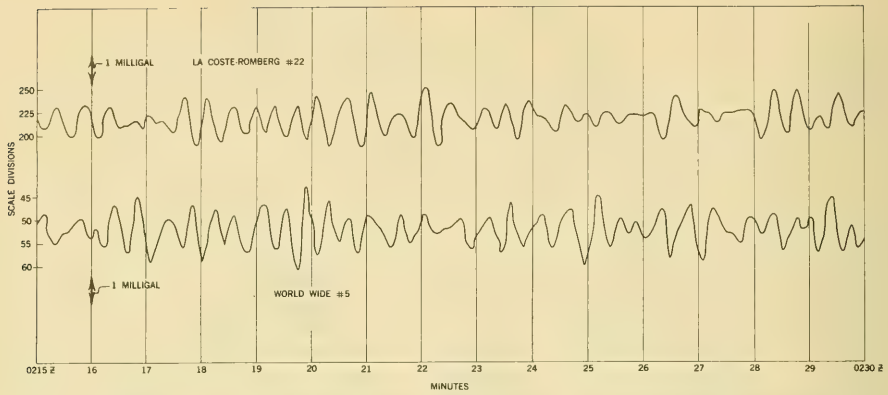

FIGURE 7 A portion of the gravimeter records taken simultaneously at ARLIS II and on the pack ice 1,240 meters distant, 3 June 1961

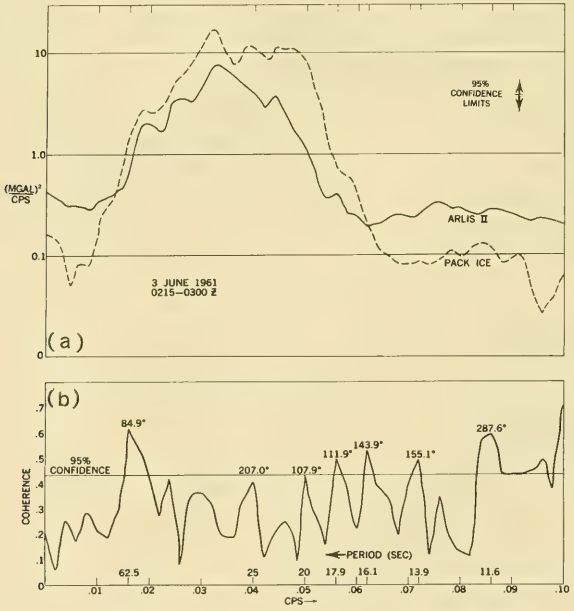

FIGURE 8 (a) Power spectra of simultaneous gravimeter records
(b) Coherences for these records

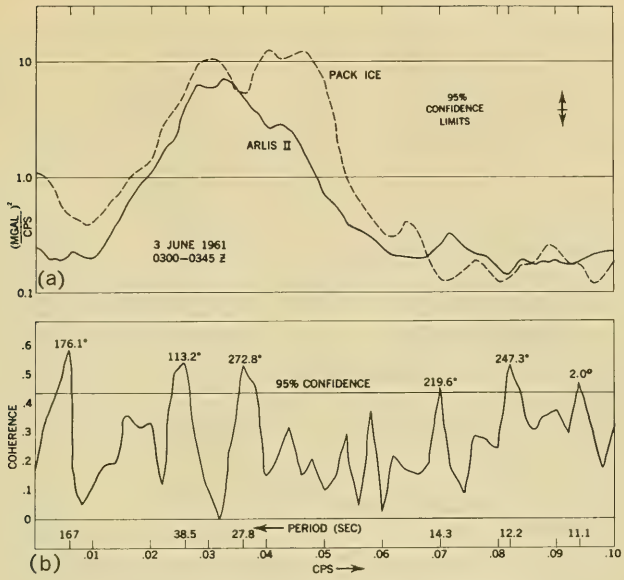

FIGURE 9 (a) Power spectra of simultaneous gravimeter records
(b) Coherences for these records

plotted in figures 8b and 9b. The same analysis described by Munk et al. (1963) for a 2-element array to measure swell in the Pacific Ocean was then applied to the present data.

b. Direction Finding

Figure 10 shows placement of the array on 3 June 1961. The phase relationships given in figures 8b and 9b show that the energy passed the north (N) station before the south (S) station. With only two elements in the array, an ambiguity of wave directions is inherent. The waves may be coming either from the west or the north. Examination of the weather maps just prior to and during the wave recording shows a strong storm system centered over Siberia (figure 11). Strong southerly winds were indicated over the western Chukchi Sea. On the other hand, the northern part of the Arctic Basin appears calm. It was therefore assumed that the observed waves were associated with the Siberian storm and were coming from the west. Consider, then, an elementary wave train of frequency f coming from a direction α measured clockwise relative to the azimuth of the normal to the array (233°T). The signals observed at the S and N gravimeters, respectively, could be written as

$$\eta_S = A \cos (2\pi ft - \phi) \quad (12)$$
$$\eta_N = A \cos (2\pi ft) \quad (13)$$

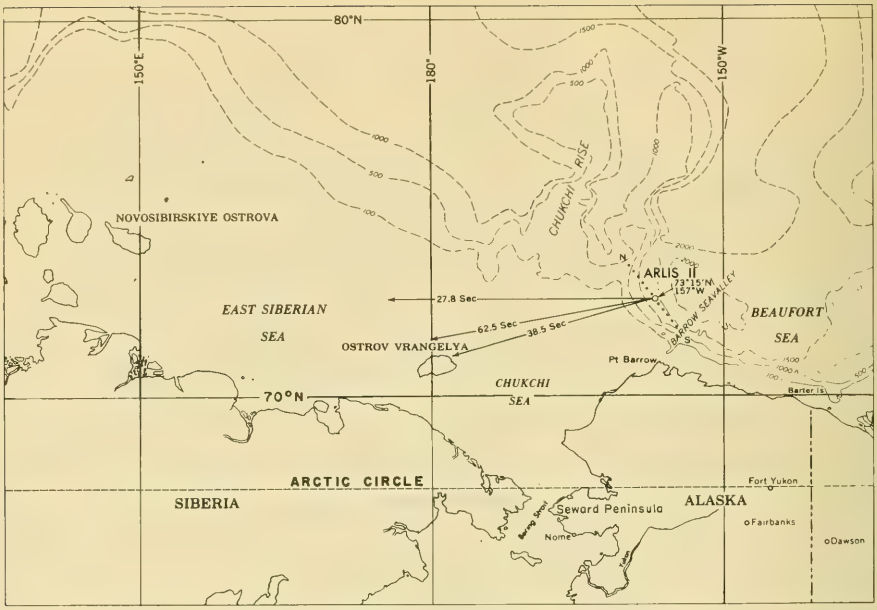

FIGURE 10 ARLIS II pack ice gravimeter array, 3 June 1961—Some computed wave paths are plotted. Depth contours in fathoms.

where $\phi = \frac{2\pi D}{\lambda} \sin \alpha$ (the phase difference)

D = distance separating instruments (1,240m)
λ = wave length

It can be seen that the same phase difference ϕ can be obtained by waves coming at an angle α as well as $180^\circ - \alpha$. The former value has been chosen as the most likely wave direction.

There is also another ambiguity inherent in the 2-element array when the observed waves are so short that the phase angle ϕ exceeds 180°. Only the principal value of ϕ, i.e., between $\pm \pi$ can be estimated. Its true value may actually be any additional multiple of 2π, and thus several values of the wave direction α can be computed according to

$$\sin \alpha_j = (\phi + 2\pi j)/(\frac{2\pi D}{\lambda}) \qquad (14)$$

where $j = 0, \pm 1, \pm 2, \cdots$, up to the largest value for which $\sin \alpha_j$ still lies between ± 1.

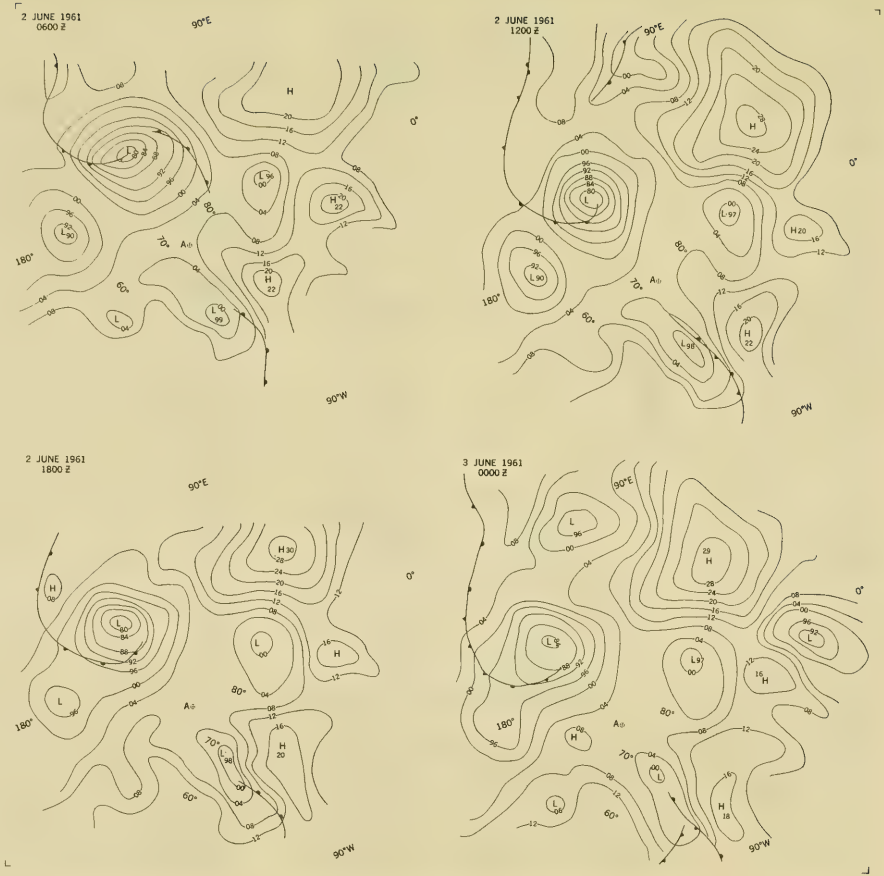

FIGURE 11 Surface weather maps, 2-3 June 1961. Contour values in millibars. Only last 2 digits given, i.e., 94 = 994 mb; 08 = 1008 mb. A = ARLIS II

In solving equation (14) the following assumptions have been made:

(1) Coherence peaks greater than 0.44 (the lower limit of the 95 percent confidence level) are assumed to be meaningful. The periods and phase angles associated with these peaks are given in figures 8b and 9b. (In one case, the 25-second peak, although falling slightly below the 95 percent confidence line, has also been used in these computations to provide continuity in the spectra.)

(2) The waves obey classical gravity wave theory. For the period range considered, it was assumed as Robin (1963) had done, that the velocities and wavelengths of the waves were essentially unaffected by ice cover.

Thus the velocity $$C = \left[\frac{g\lambda}{2\pi} \tanh \frac{2\pi H}{\lambda}\right]^{1/2} \quad (15)$$

and $$\lambda = \lambda_d \left[\tanh \frac{2\pi H}{\lambda_d}\right]^{1/2} \quad (16)$$

where C = wave velocity (m/sec)
g = gravity (9.83 m/sec^2)
H = water depth(m)
$\lambda_d = \frac{gT^2}{2\pi}$
T = period (sec)

(3) Although the array was located in deep water (approximately 1,600m) the presumed direction of incoming waves was across the wide and shallow continental shelf north of Siberia. Since tne greatest portion of the total distance traveled was across this shelf, an average depth of 150m was used in the computations of λ .

The solutions for α computed from equation (14) and corresponding to waves from the west are plotted in figure 12. The values of α for periods of 25 seconds or more are unique. As the wave periods become shorter than 25 seconds, two, three, four, and finally five solutions become possible. For periods shorter than 25 seconds, there is no real guide for the choice of solution or solutions. In the analysis of Munk et al. (1963), the extension of the unique solutions, i.e., when $j = 0$, was preferred, because a sense of continuity was maintained. This was justified because their plot of coherences vs frequency, upon which their solutions of α were based, was itself fairly continuous. No such continuity was observed in the plot of coherences versus frequency in this study, rather there were discrete coherence peaks emerging from the noise level. Thus, it appears just as likely to have short-period solutions of α coming from the higher order branches as from the $j = 0$ branch. This problem cannot be resolved without an additional element in the array.

The peak at 167-second period (figure 9b) poses an interesting problem. With its computed phase angle of 176° no solution of equation (14) exists.

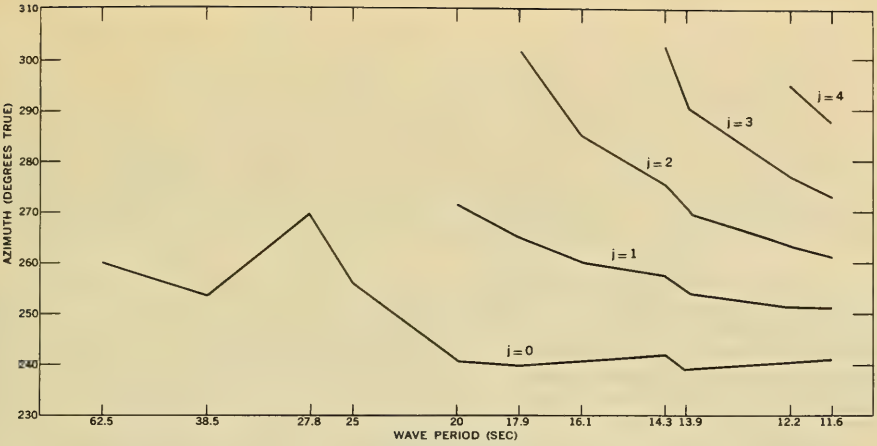

FIGURE 12 Computed wave directions as a function of period—3 June 1961, 0215—0345Z

Since all other values appear fairly continuous in azimuth, it has been assumed that some other mechanism or mode of propagation is responsible for its existence. If it were due to some instrument characteristics or a fault of the digitizing process, one might expect to find the peak in both records; however, it appears only in the 0300 to 0345Z record. If the peak is real and not extraneous, it may well have been caused by an earthquake. The records show an earthquake of magnitude $5\frac{1}{4}$ to $5\frac{1}{2}$ occurring at 0100 hrs, 13 min, 25.4 sec at a depth of about 29km near Kamchatka (53.3°N,164.8°E) on this date. The W_2, second arrival (via the antipodes) of seismic surface waves of the "G" type, would fall within the 0300 to 0345Z record interval. Such waves have periods of from 1 to 4 minutes, and multiple arrivals are often observed (Richter, 1958). Such energy could be imparted to the shorefast ice cover at many points along its periphery and conceivably produce the observed response of 167-second period at the array.

c. Beam Width

As shown in Munk et al. (1963), the value for coherence may be used as an indication of the beam width of the incoming waves. They give the following equation for determining the beam width.

$$\Delta\alpha = (1 - R^2)^{1/2}/(\frac{\pi D}{\lambda} \cos \alpha) \qquad (17)$$

where $\Delta\alpha$ = beam width
R = coherence
$\sin\alpha = \phi/\frac{(2\pi D)}{\lambda}$
ϕ = phase angle

Values of $\Delta\alpha$ for periods of 62.5, 38.5, and 27.8 seconds are about 30°, 20°, and 15°, respectively. These beam widths seem quite believable when the proximity and width of the storm are taken into account.

d. Evaluation of the Results of the 2-Element Array

Probably the most significant conclusions that can be drawn from this experiment are (1) that waves in the Arctic are generated by storms as are waves in the open ocean, (2) that they can propagate over substantial distances (350 nautical miles or more in this case), and (3) that the wave directions can be determined with a multielement array and cross-correlation techniques.

The actual values obtained for wave directions and beam width must be regarded with caution for, in addition to the ambiguity introduced by using only two elements, the values are dependent upon variables that were not well known. The waves were assumed to travel at velocities calculated according to gravity wave formulas applicable in the open ocean. This assumption was probably valid for waves recorded on the thin pack ice, particularly at the long-period end of the spectrum. Waves traveling through the thicker ice of ARLIS II, however, may have velocities different from those assumed, especially at the short-period end of the spectrum. These shorter waves approach the flexural waves discussed by Ewing and Crary (1934) and by Hunkins (1962). More detailed knowledge of the thickness of ARLIS II, the water depths beneath the stations and along the wave paths, and the effects of the ARLIS II-pack ice boundary would be required for a more accurate analysis.

The values for the three longest period waves are therefore probably most correct, because they were obtained with the least ambiguity of solutions, are least likely to be affected by refraction and boundary effects of ARLIS II and the pack ice, and are least affected by errors due to recording and digitizing processes.

For future experiments, at least three instruments should be used with a spacing of no more than 300 meters on the thinnest pack ice possible and in deep water. It is expected that many of the problems discussed above would be avoided by adhering to these conditions.

5. SIMULTANEOUS WAVE AND PRESSURE SPECTRA BEFORE, DURING, AND AFTER A STORM

a. Introduction

Since it was clear that some relationship existed between the wind above the ice and the waves beneath, several simultaneous sets of micropressure and wave records were examined. The windspeed and direction graph for July 1961 (figure 13) suggested a particularly good time interval between 5 and 6 July for such a study. During this interval, the windspeed increased from 12 to 25 knots and decreased to 12 knots in the next interval of the same duration. This corresponds to the approach and passing of a storm (figures 14 and 15). Five 90-minute intervals, 5 hours apart, were selected for this analysis. The records are shown in figures 4a, b, and c.

b. Microbarograph Records

It was assumed that a moving load mechanism similar to the type suggested by Sytinskiy and Tripol'nikov (1964) was the primary cause of the waves. Thus the microbarograph, which measures directly the oscillatory loading of the

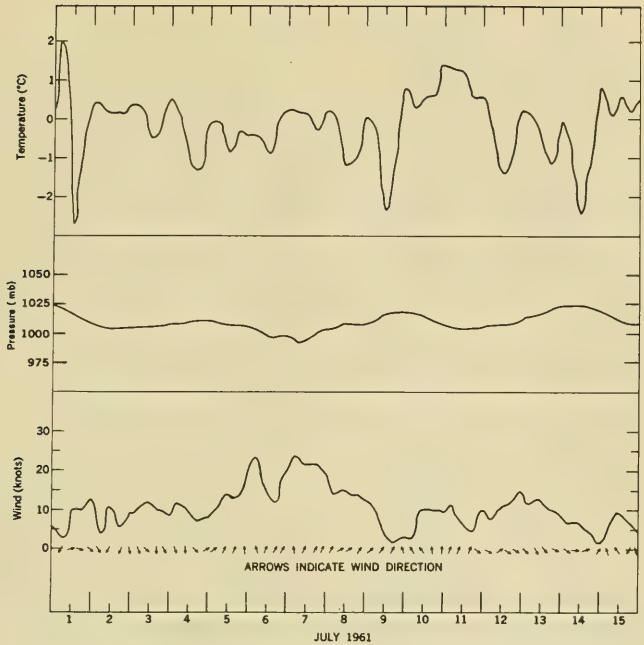

FIGURE 13 Surface weather conditions, ARLIS II, 1—15 July 1961

ice by atmospheric pressure, is well adapted for this study. Power spectra for each of the five 90-minute intervals were computed, corrected for instrument response, and plotted in figure 16. A low lag number (20) was used to increase the accuracy of spectral estimates. The most noticeable characteristics of spectra plotted on the same set of coordinates are close dependence of power density on local windspeed at all periods and increase of power density with period. Even with the low resolution used in this example, distinct peaks appear and are probably real; instead of appearing to follow a set pattern, they shift slowly with time as mentioned in section 3(d).

Very little is known about the properties of these short-period pressure waves — whether they are in fact progressive waves and, if so, how fast they propagate. Waves similar to these have been observed on land by Flauraud et al. (1954) while studying micropressure waves with periods of 5 to 100 minutes with a tripartite array in the Boston area. Waves of 5- to 100-minute periods propagated with velocities of 20 to 175 knots and were correlated with winds at the 200-mb level. Wave periods less than 10 minutes were not conservative over the length of the array (6 to 9 miles), thus little was learned about their propagation characteristics. Martyn (1950) showed that micropressure

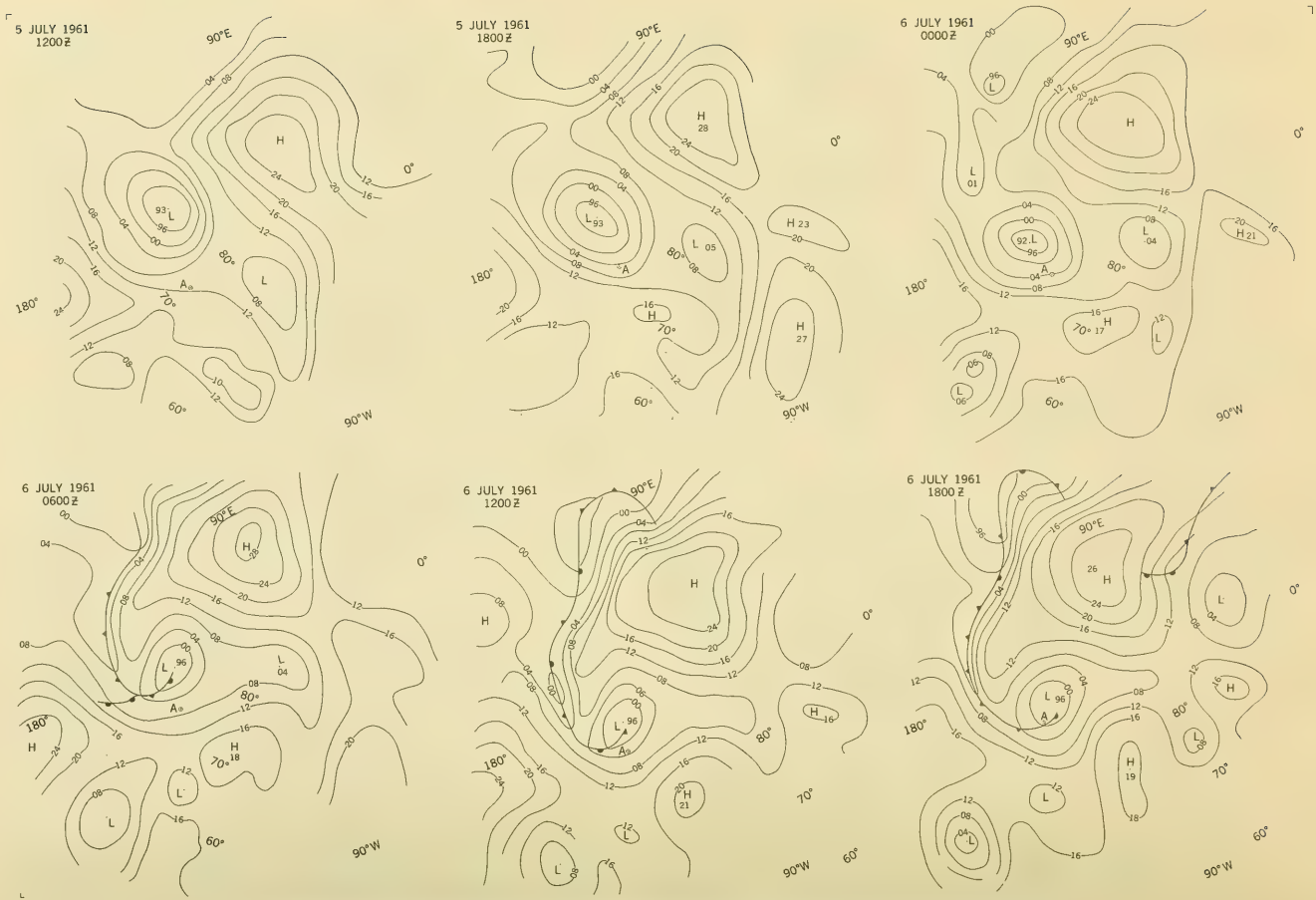

FIGURE 14 Surface weather maps, 5-6 July 1961. Contour values in millibars. Only last 2 digits given, i.e., 94 = 994 mb; 08 = 1008 mb. A = ARLIS II

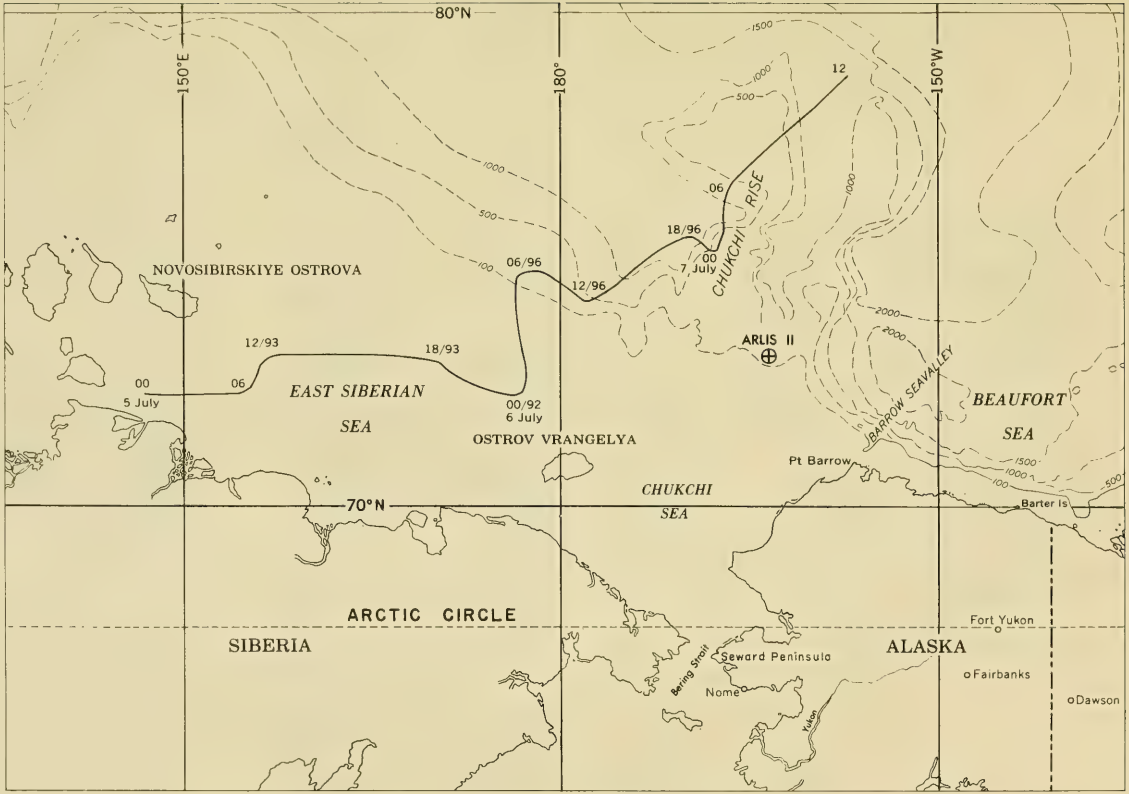

FIGURE 15 Track of storm center 5—7 July 1961, plotted at 00, 06, 12, and 18Z each day—Pressures at storm center are in millibars (96 = 996). Depth contours in fathoms.

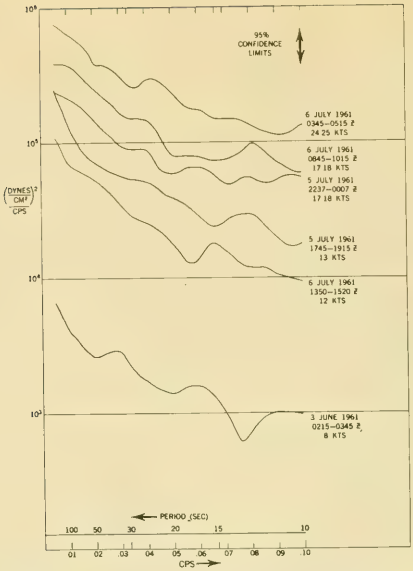

FIGURE 16 Power spectra of six 90-minute microbarograph records—Spectra are corrected for instrument response.

oscillations could be generated by vertical wind shear in a horizontal atmospheric duct bounded on the bottom by the ground and on the top by a temperature discontinuity. Such ducts occur frequently in the Arctic; however, the period of this generating mechanism has a theoretical lower limit of about 10 minutes.

In any event 10- to 100-second micropressure waves exist in the Arctic. As will be shown later, these micropressure waves have sufficient energy to bend the ice and generate water waves. It has been assumed that micropressure waves propagate in the same direction as the wind. The nature of these waves in an area for much further study.

c. Gravimeter Records

Low resolution power spectra for the five wave records taken during 5 and 6 July were computed, corrected for instrument response, and plotted on the same set of coordinates (figure 17).

Dispersion of long-period waves traveling from a distant source and local generation of short-period waves are clearly displayed in this figure.

(1) The effects of wave dispersion are seen for periods longer than 16 seconds. Long-period energy (60 or more seconds) in the 1745 to 1915Z record increases 6 to 7 times in magnitude 5 hours later in the 2237 to 0007Z

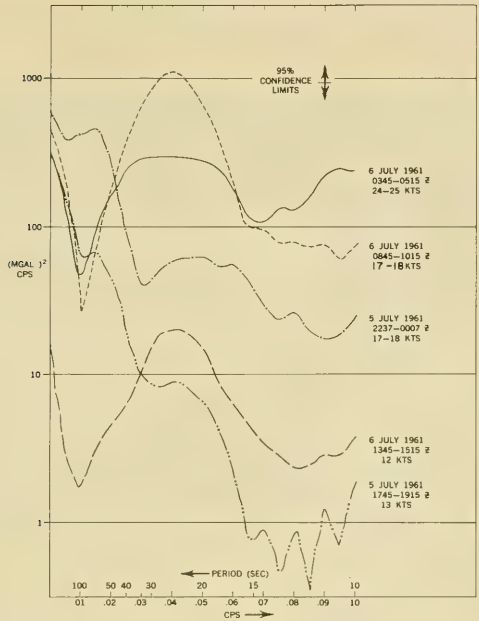

FIGURE 17 Power spectra of five 90-minute gravimeter records taken during 5 and 6 July 1961—Spectra are corrected for instrument response.

record. This long-period buildup can easily be seen by examining the first two records. The long-period, high amplitude waves can be seen clearly on the 2237 to 0007Z record (figure 4a). Five hours later, between 0345 and 0515Z, this long-period energy has disappeared, and energy between 20- and 40-second periods has increased considerably. Later, between 0845 and 1015Z and well after the storm's peak, energy of about 25-second period has increased 2 to 3 times in magnitude; the long-period energy has essentially disappeared in this record. Ten hours after the storm's peak, the overall energy has been substantially reduced.

(2) Through examination of energy with periods less than 16 seconds, the direct dependency of wave energy on local surface windspeed is readily observed. This dependence was previously reported by Sytinskiy and Tripol'nikov (1964) and Hunkins (1962). Hunkins noted that there appeared to be some threshold velocity above which the wind excited the ice and suggested a value between 20 and 24 knots. It appears from figure 17 that such a threshold velocity in this case is at or below 12 or 13 knots. ARLIS II, however, is a special case, since it is considerably thicker than the pack on which the above two studies were conducted. Thus, the short-period energy that appears so dependent upon the wind is probably the natural bobbing of the ice island as computed

according to equation (1), where ρ = ice density ($0.90 gm/cm^3$), ρ' = water density ($1.025 gm/cm^3$), and g = gravity ($983 cm/sec^2$).

For ice 20 meters thick (the estimated thickness of ARLIS II), T = 8.5 seconds; T increases to 14.7 seconds for ice thickness of 60 meters. Short-period spectral peaks of all curves in figure 17 lie between 10 and 14 seconds. To examine this period range more closely, a portion of the 0345 to 0515Z wave record was used to recompute the power spectrum using a $\triangle T$ of 2.5 seconds (figure 18). This permits the extension of the short-period end of the spectrum

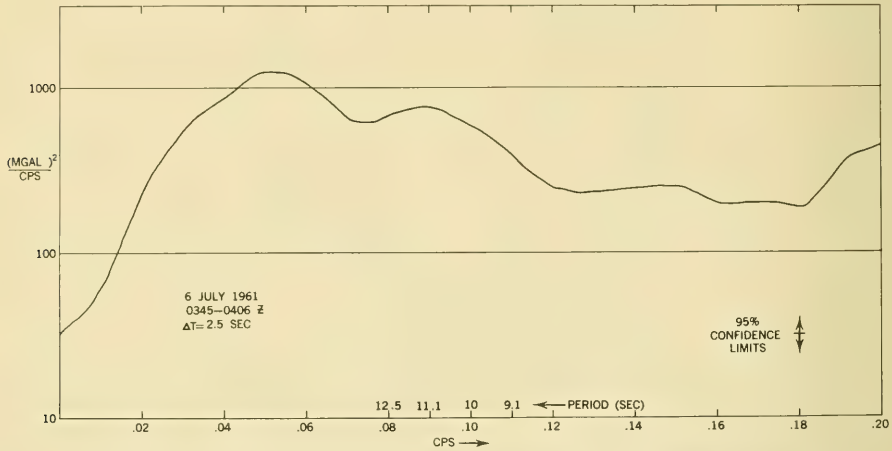

FIGURE 18 Power spectrum of a portion of the 0345—0515Z gravimeter record emphasizing short-period energy.

from a minimum of 10 seconds to 5 seconds. The peak at 11.1 seconds appears real and probably is the natural oscillation of the island excited by the wind. When simultaneous wave recordings were made on ARLIS II and the adjacent pack, this short-period resonant energy was notably lacking in the pack ice record, while long-period energy levels were more nearly alike. Spectra computed from these records and corrected for instrument response are compared in figure 19.

Further evidence of this natural bobbing is obtained by close examination of the high amplitude arrivals in the long wave record shown in figure 20. The three such arrivals shown have average periods of 9.7, 10.9, and 12.5 seconds. The increased energy at 2035:10 is shown on an expanded scale in figure 21. It was assumed that this energy was imparted by collision of the island with adjacent floes. The comparatively slow decay of this energy suggests that there is little damping action in this ice-water system.

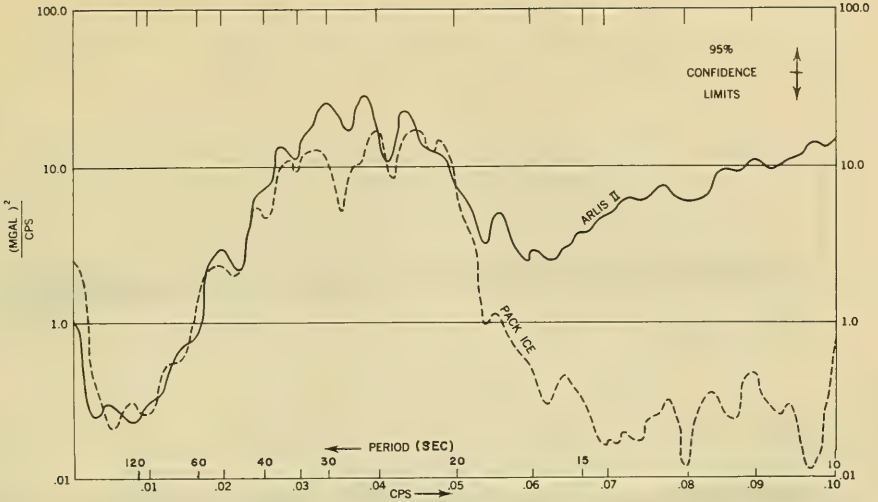

FIGURE 19 A comparison of power spectra of simultaneous gravimeter records, 0215—0345Z, 3 June 1961—Spectra are corrected for instrument response.

6. DISCUSSION

a. The Relationship of Atmospheric Micropressure Fluctuations to Water Waves

Cross-correlations of many of the simultaneous wave and micropressure records were computed to see if quantitative relationships could be determined. The coherences of these paired records are plotted in figure 22 and meaningful peaks are observed. The coherence values of the peaks seem to have no relationship to local wind velocity but appear to be a function of the average local surface wind direction. This can be seen when the coherences of the significant peaks are plotted against the average wind direction observed at the time the records were made (figure 23). Maximum coherences occurred when the wind direction was about 185°T, suggesting that maximum wind-to-wave energy transfer occurs at this location when the wind blows from this direction.

The dependency on direction could be explained in the following manner. Since the pack ice pressure ridge systems in this area of the Beaufort Sea had a general east-west trend during this time (Wittmann, 1964), they would offer the greatest resistance to forces moving in a generally north-south direction. Considerably more observations, however, are needed to verify such an hypothesis.

Significant coherences appear only with waves generated at some distance from the recording site. As would be expected, there is no coherence between local wind and the wave motion due to the resonant period of ARLIS II.

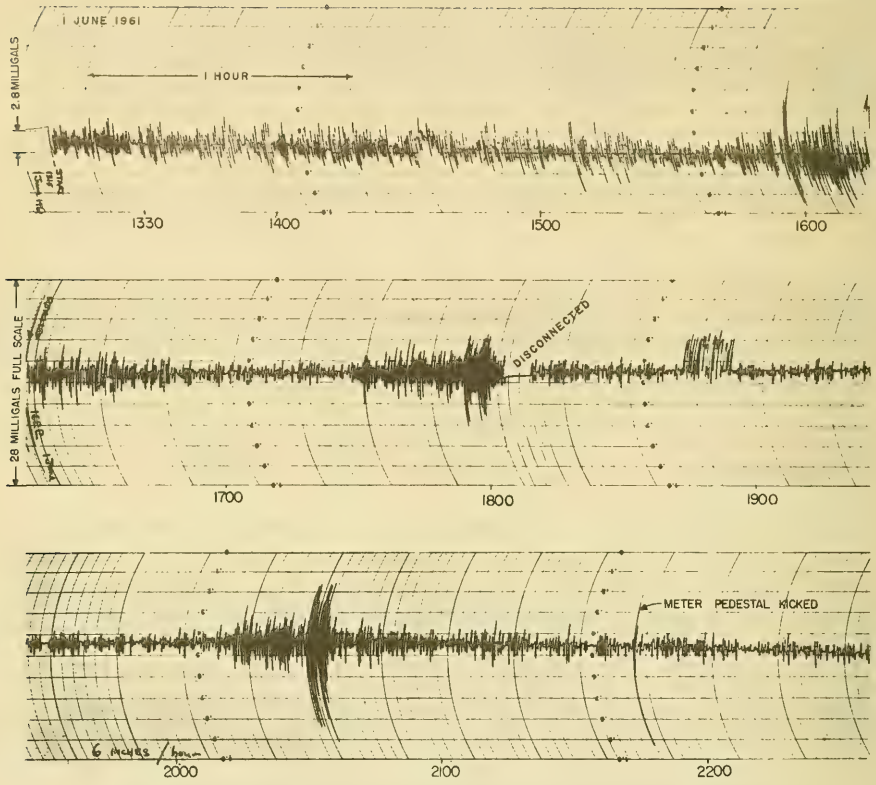

FIGURE 20 Nine-hour gravimeter recording beginning 1315 local time (2315Z) 1 June 1961 on ARLIS II

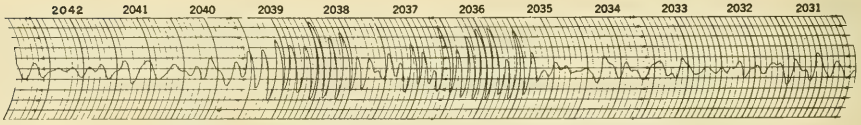

FIGURE 21 Expansion of high-amplitude, short-period event shown in figure 20

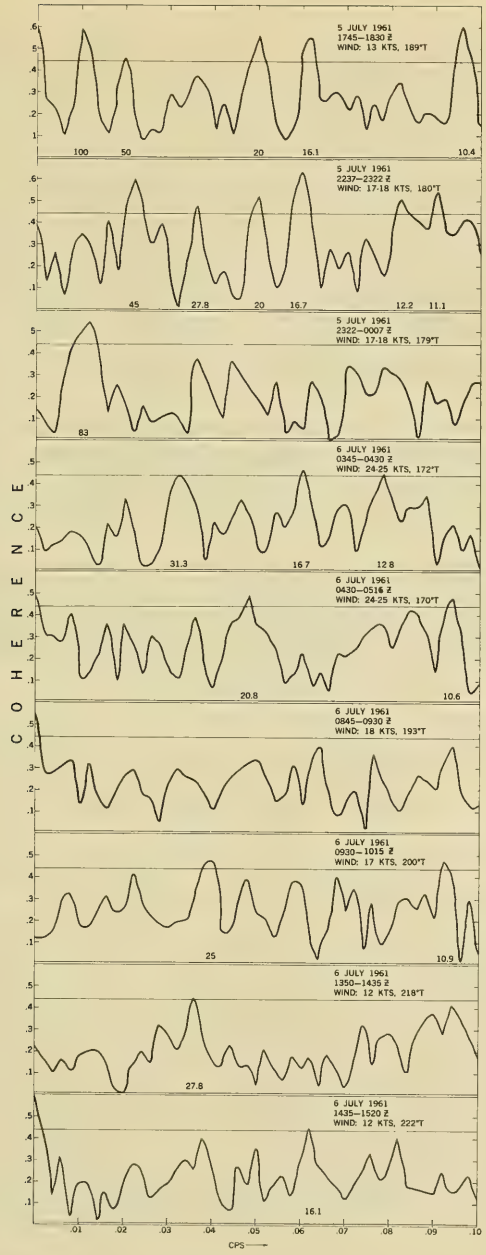

FIGURE 22 Coherence as a function of period for five simultaneous 90-minute microbarograph and gravimeter records, 5-6 July 1961—Windspeeds and directions are average. Line at 0.44 coherence is 95 percent confidence limit.

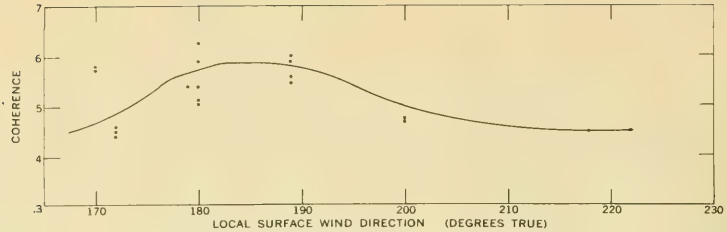

FIGURE 23 Significant coherences from figure 22 plotted against average surface wind direction observed during the recording interval.

b. Energy Transfer Considerations

Sections 4 and 6a above indicate that the waves are generated in a storm area and are selectively reinforced by micropressure waves acting through the ice along the path of the ocean waves. It would be interesting, therefore, to determine the relationship of micropressure wave force to the force required to bend the ice and generate ocean waves.

It should be shown first that the ice will indeed behave elastically for the ice thicknesses and wave periods and amplitudes involved. Following Robin (1963), a rough calculation can be made of the stresses involved in bending an ice plate of thickness h into the form expressed by:

$$y = A \sin (2\pi \frac{x}{\lambda}) \tag{18}$$

If elastic bending occurs about a neutral plane in the center of the plate, the surface stress σ_{xs} is given by

$$\sigma_{xs} = \frac{Mh}{2I} \tag{19}$$

where M is the bending moment at any point, and $I = \int_{-1/2h}^{1/2h} y^2 dy$

$$\text{Since } M = \frac{EI}{(1 - \mu^2)} \frac{d^2y}{dx^2} \tag{20}$$

where E = Young's modulus, and μ = Poisson's ratio, an expression for σ_{xs} can be made by combining equations (18), (19), and (20) so that

$$\sigma_{xs} = \frac{E}{(1 - \mu^2)} \frac{h}{2} A \frac{4\pi^2}{\lambda^2} \sin (2\pi \frac{x}{\lambda}) \tag{21}$$

This should be evaluated at both ends of the wave spectrum being considered, since the values of A and λ vary considerably over this range. It should also be evaluated for ARLIS II (20m thick) as well as for the pack ice (2m thick).

Figure 24 shows the "displacement" spectra computed from the "acceleration" spectra in figure 17 and plotted in terms of twice the mean wave amplitude squared per frequency bandwidth. Representative amplitude maxima for observed long- and short-period waves were taken from this plot and used for evaluating equation (21).

The values chosen were for periods of 67 seconds (2237 to 0007Z) and 11.1 seconds (0345 to 0515Z). These correspond to average amplitudes of 1.86cm and 0.032cm, respectively. For these periods the following sets of values were used:

T = 67 sec	T = 11.1 sec
λ = 2,560m (shallow water wavelength)	λ = 193m
A = 1.86cm	A = 0.032cm
h = 2m, 20m	h = 2m, 20m
μ = 0.3	μ = 0.3

Although Robin used 5×10^{10} dynes/cm^2 as an approximate value for E (Young's modulus for sea ice), more recent data suggest that 1×10^{11} dynes/cm^2 is probably closer to the actual value for sea ice, particularly for ARLIS II ice (Langleben and Pounder, 1963).

From these values, the following maximum stresses were obtained:

For T = 67 sec
$\sigma_{xs} = 1.23 \times 10^4$ dynes/cm^2 for ice 2m thick and
$= 1.23 \times 10^5$ dynes/cm^2 for ice 20m thick.

For T = 11.1 sec
$\sigma_{xs} = 3.72 \times 10^4$ dynes/cm^2 for ice 2m thick and
$= 3.72 \times 10^5$ dynes/cm^2 for ice 20m thick.

These values are considerably less than 2.2 to 3.9×10^6 dynes/cm^2, the range of stresses that Butkovich (1956) found were required to fracture sea ice beams under similar conditions in the laboratory. Tabata (1955) indicated that the major part of sea ice deformation would be elastic under short-period stresses. It is therefore reasonable to conclude, in the same manner as Robin, that the ice can be treated as an elastic plate for all wave amplitudes and periods encountered in this experiment.

It is now desirable to see if the micropressure waves in fact have sufficient vertical force to bend the ice and generate waves beneath it. In order to do this, it is necessary to show that the oscillating vertical pressure on the ice is enough to bend the ice at least as much as the gravimeter records for that particular period.

Only the pack ice system will be considered in this connection, for

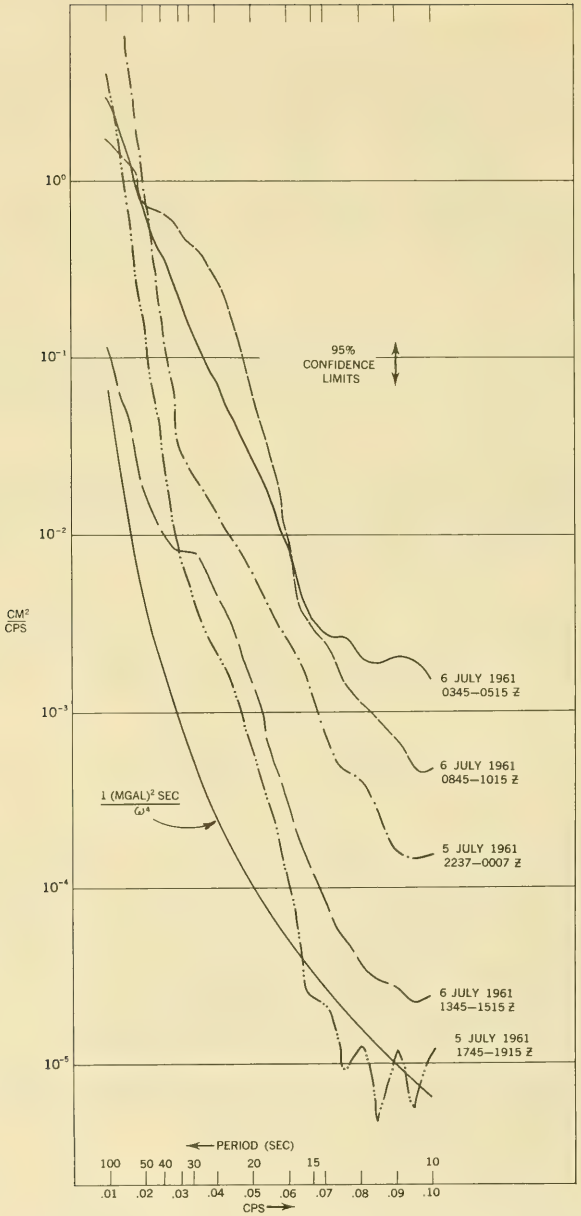

FIGURE 24 "Displacement" power spectra computed from the "acceleration" spectra shown in figure 17.

it alone is representative of the Arctic Ocean Basin. The thick ice island is an anomaly and, especially because of its resonance, appears to behave differently than the pack.

The vertical pressure σ_y needed to bend an elastic plate of thickness h is given by

$$\sigma_y = \frac{-Eh^3}{12(1 - \mu^2)} \frac{d^4y}{dx^4} \tag{22}$$

If the plate is bent about a central plane into the form of equation (18) then

$$\sigma_y = \frac{-4Eh^3 \pi^4}{3(1 - \mu^2)\lambda^4} A \sin\left(2\pi \frac{x}{\lambda}\right) \tag{23}$$

Computations of σ_y for a short-period component appear most useful because: (1) the required bending pressure will generally be greater, the shorter the period; and (2) the shorter period waves are more likely to have been generated closer to the recording site owing to the significant attenuation that they undergo (α 1/ λ^4) compared to the longer periods. Furthermore, it appears from section 6a above that atmospheric energy can be added along the wave path. Presumably, then, the shorter the wave period, the shorter the distance between generating area and receiving site. Therefore, comparison of the force of the short-period micropressure waves with the short-period ocean waves would probably be most meaningful.

From figure 25 showing the "displacement" spectra of the two simultaneous time series, the 11.1-second ocean wave component was calculated to induce an average displacement of the pack ice of 0.001cm between 0215 and 0345Z. For a wave period of 11.1 seconds, λ = 193m, and the maximum stress necessary to bend the ice (from equation (23)) is 0.8 dynes/cm^2.

From figure 16, the 11.1-second component of the micropressure spectrum (0215 to 0345Z, 3 June 1961) was found to have an average value of 22.4 dynes/cm^2 or 28 times the theoretical force necessary to bend the ice sinusoidally with the observed displacement. This rough calculation suggests that there is ample energy in the micropressure waves to completely explain the water water generation beneath the ice, even at relatively low wind speeds (8 knots in this case).

7. CONCLUSIONS AND RECOMMENDATIONS FOR FURTHER WORK

Waves of the swell type are generated in the Arctic Ocean Basin and are associated with storms as are those in the open ocean. The thin, elastic ice cover in the Arctic limits considerably the maximum amplitude that the swell can have and drastically attenuates waves in the period range usually

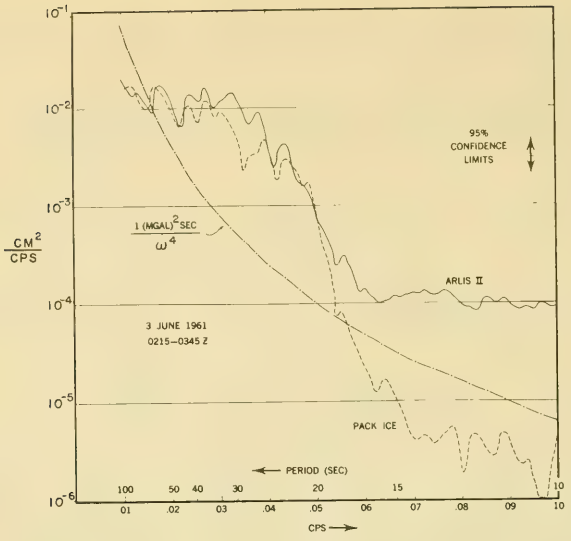

FIGURE 25 "Displacement" power spectra computed from the "acceleration" spectra shown in figure 19.

observed on the open ocean.

This swell is directional and can be satisfactorily measured by an array of gravimeters placed on the ice. The major portion of the wave energy is probably derived from storms. However, cross-correlation between micropressure waves and ocean waves at a point outside the major generating area suggests that additional energy is imparted to ocean waves outside of this area. Cross-correlation of several micropressure and wave records over an interval when the average local surface wind was changing indicates that maximum coherence (and presumably maximum coupling) is a function of wind direction. This in turn suggests that local surface characteristics of the ice influence the amount of energy coupling for a given area and wind direction.

If it is assumed that micropressure wave spectra everywhere over the Arctic Ocean are similar to the ones measured at ARLIS II, varying primarily as a function of wind velocity, then the total energy of a water wave at a given point is probably related to an integration of all the atmospheric energy surrounding that point. This would explain the continual wave interference observed at the tripartite array of Sytinskiy and Tripol'nikov (1964). In addition to observing waves generated by a storm, there would also be observed the effects of the micropressure wave system acting like so many small storms, each contributing energy to the water.

Waves from distant sources show typical dispersion patterns, the long

periods arriving before the short periods. No attempt was made to estimate the point of origin of these waves by relating their group velocities and times of arrival as Munk et al. (1963) had done, because the sources were too close and too wide to assume a point source origin necessary for such calculations.

The moving-load-resonant-plate theory of Sytinskiy and Tripol'nikov could not be adequately tested, because the range of periods that they associated with a water depth of 150m (12 to 15 seconds) is masked by the natural free oscillation of ARLIS II. It appears, however, that there is sufficient energy in the micropressure waves alone to cause water waves having these periods simply by sympathetic vibration.

The work discussed so far suggests several further investigations both in the Arctic Ocean Basin and in the open ocean. A tripartite gravimeter array, approximately 300 meters on a side, should be established on pack ice in deep water somewhere in the central Arctic Ocean Basin. At each station there should also be a microbarograph and provision for recording surface wind velocity continuously. The gravimeter and microbarograph data should be recorded digitally in a form that could be fed directly into a computer. Analog output alone should not be considered owing to the immense task involved in converting it to digital form. If gravimeter recordings are continuous, waves generated anywhere in the Arctic Ocean Basin would be recorded. Their sources could also be determined.

Similarly, the three-dimensionality and propagation characteristics of the micropressure waves could be studied with the microbarograph array. Finally, cross-correlations between the two phenomena should be useful in determining quantitatively air-sea energy transfer relationships as a function of wave period. Many of these findings would probably apply to the open ocean as well.

Such a study could provide statistical information on wave directions and might provide information on ice breakup due especially to what Assur (1963) calls "long-wave cracks".

Since the micropressure waves described here have been observed elsewhere, it is probable that they would be observed over the open ocean also. A station might very profitably be established on a stable platform such as ARGUS ISLAND near Bermuda.

ACKNOWLEDGEMENTS

This study was a special project jointly supported by the U.S. Naval Oceanographic Office and the Office of Naval Research. The Oceanographic Office provided the LaCoste-Romberg gravimeter and supported the data reduction. The Office of Naval Research provided logistic support through its Arctic Research Laboratory at Barrow, Alaska. The Geophysical and Polar Research Center, University of Wisconsin, provided the World-Wide gravimeter. The T-21 microbarograph was generously loaned by the Terrestrial Sciences Laboratory of the Air Force Cambridge Research Laboratories.

Particular thanks go to Dr. Ned A. Ostenso of the Geophysical and Polar Research Center, who assisted in the organization of the field program and encouraged the author to use this work as a thesis project; to Mr. John J. Schule, Jr., Head of the Oceanographic Prediction Division of the Oceanographic Office, whose continued interest in and support of this project made it possible; and to Mr. William McComas of the same office who assisted in much of the data collection.

Thanks are also given to the following persons whose personal interest and assistance in this project are greatly appreciated: at the Oceanographic Office, Mr. Robert J. Beaton, Director, Nautical Chart Division; Mr. Albert L. McCahan, Head, Gravity Branch; and Mr. Walter I. Wittmann, Head, Arctic Section. Appreciation is also expressed for the help provided by Dr. Max E. Britton, Head of the Arctic Project at the Office of Naval Research, Mr. Max C. Brewer, Director of the Arctic Research Laboratory, and Mrs. Elisabeth Iliff of the Air Force Cambridge Research Laboratories.

The author acknowledges with pleasure the assistance of colleagues at the Oceanographic Office, particularly Dr. Lloyd Simpson, and Messrs. P. S. DeLeonibus, Tim Barnett, Lionel Moskowitz, and David Amstutz who provided much help during the project and critically reviewed the final manuscript.

REFERENCES

Assur, A., Breakup of Pack Ice Floes, in Ice and Snow, Edited by W. D. Kingery, 335-347, The M.I.T. Press, Cambridge, 1963.

Blackman, R. B., and J. W. Tukey, The Measurement of Power Spectra, Dover, New York, 1958.

Butkovich, T. R., Strength Studies of Sea Ice, S.I.P.R.E. Res. Rep., No. 20, Corps of Engineers, U.S. Army, 1956.

Crary, A. P., R. D. Cotell, and J. Oliver, Geophysical Studies in the Beaufort Sea, 1951, Trans. Am. Geophys. Union, 33, 211-216, 1952.

Crary, A. P., and N. Goldstein, Geophysical Studies in the Arctic Ocean, A.F.C.R.C. Geophysical Research Papers, No. 63, A.F.C.R.C.-TR-59-232(1), Vol. 1, 7-30, 183-218, 1959.
(This paper was originally published in Deep-Sea Research 4, 185-201, 1957. The cited reference is used, however, since it contains many valuable data in the appendix not available in the earlier publication.)

Ewing, M., and A. P. Crary, Propagation of Elastic Waves in Ice, 2, Physics, 5, 181-184, 1934.

Flauraud, E. A., A. H. Mears, F. A. Crowley, Jr. and A. P. Crary, Investigation of Microbarometric Oscillations in Eastern Massachusetts, A.F.C.R.C. Geophysical Research Paper, No. 27, A.F.C.R.C. Technical Report 54-11, 1954.

Hunkins, K., Waves on the Arctic Ocean, J. Geophys. Res., 67, 2477-2489, 1962.

Langleben, M. P. and E. R. Pounder, Elastic Parameters of Sea Ice, in Ice and Snow, Edited by W. D. Kingery, 69-78, The M.I.T. Press, Cambridge, 1963.

LeSchack, L. A., ARLIS II: New Arctic Drift Station, Naval Res. Rev., Sept., 12-18, 1961.

LeSchack, L. A. and R. A. Haubrich, Observations of Waves on an Ice-Covered Ocean, J. Geophys. Res., 69, 3815-3821, 1964.

Martyn, D. F., Cellular Atmospheric Waves in the Ionosphere and Troposphere Proc. Roy. Soc., London, A. 201, 216-234, 1950.

Munk, W. H., F. E. Snodgrass and M. J. Tucker, Spectra of Low-Frequency Ocean Waves, Bull. Scripps Inst. Oceanogr., University of California, 7, 4, 283-362, 1959.

Munk, W. H., G. K. Miller, F. E. Snodgrass, and N. F. Barber, Directional Recording of Swell From Distant Storms, Phil. Trans. Roy. Soc., London, A, 255, 505-589, 1963.

Nettleton, L. L., Geophysical Prospecting for Oil, McGraw-Hill Book Company, New York, 1940.

Richter, C. F., Elementary Seismology, W. H. Freeman and Company, San Francisco, 1958.

Robin, G. de Q., Wave Propagation Through Fields of Pack Ice, Phil. Trans. Roy. Soc., London, A, 255, 313-339, 1963.

Sytinskiy, A. D. and V. P. Tripol'nikov, Some Results of Investigations of Natural Oscillations in the Ice Fields of the Central Arctic, Izv. Akad. Nauk, SSSR, Ser. Geophys., 4, 615-621, 1964.

Tabata, T., A Measurement of Visco-Elastic Constants of Sea Ice, J. Oceanogr. Soc. Japan, 11, 185-189, 1955.

Wittmann, W. I., Pers. Comm., 1964.

UNCLASSIFIED

Security Classification

DOCUMENT CONTROL DATA - R&D

(Security classification of title, body of abstract and indexing annotation must be entered when the overall report is classified)

1. ORIGINATING ACTIVITY *(Corporate author)*
U.S. Naval Oceanographic Office
Oceanographic Prediction Division
Washington, D.C. 20390

2a. REPORT SECURITY CLASSIFICATION
None

2b GROUP
n/a

3 REPORT TITLE

ON THE GENERATION AND DIRECTIONAL RECORDING OF WAVES IN THE ARCTIC OCEAN (U)

4 DESCRIPTIVE NOTES *(Type of report and inclusive dates)*
Exploratory Development

5. AUTHOR(S) *(Last name, first name, initial)*

LESCHACK, LEONARD A.

6. REPORT DATE	7a. TOTAL NO. OF PAGES	7b. NO. OF REFS
SEPT. 1965	44	20

8a. CONTRACT OR GRANT NO.	9a. ORIGINATOR'S REPORT NUMBER(S)
n/a	
b. PROJECT NO. HF-103-08-02	TR-179
c 636 (Ice Prediction)	9b. OTHER REPORT NO(S) *(Any other numbers that may be assigned this report)*
d.	None

10. AVAILABILITY/LIMITATION NOTICES All distribution of this publication is controlled. Qualified DDC users shall submit requests for copies to the: Commander, U.S. Naval Oceanographic Office, Washington, D.C., 20390, ATTN: Code 4000.

11. SUPPLEMENTARY NOTES	12. SPONSORING MILITARY ACTIVITY
	U.S. Naval Oceanographic Office Washington, D.C. 20390

13 ABSTRACT

An experiment to investigate the directional nature and the possible generation mechanisms for waves on the Arctic Ocean, an ocean almost entirely covered with sea ice, is described. The waves under consideration have periods between 10 and 100 seconds and amplitudes between 0.001 and 2.0 centimeters. These waves have been previously observed with gravimeters and seismographs and have been described in the literature. (U).

In the present work an array of two continuously recording gravimeters 1,240m apart was established at drift station ARLIS II. The records obtained were examined by cross-spectrum analysis techniques. Observed waves with distinct periods were associated with a storm over Siberia. (U)

A continuously recording microbarograph sensitive to atmospheric micropressure oscillations in the 10- to 100-second period range was also installed at ARLIS II. Distinct oscillations were observed in this period range having amplitude of from 20 to 400 dynes/cm^2. Power spectra of micropressure records made before, during, and after a storm show that the oscillation amplitude is proportional to the period of the oscillation and speed of local winds. Cross correlation between the micropressure records and wave records taken with a gravimeter at the same location as the microbarograph shows a positive correlation between the micropressure waves and the ocean waves. This correlation appears to vary with the direction of the local surface wind and may be related to the orientation of pressure ridges in the ice pack. Although the nature of the micropressure oscillations could not be determined with only the one sensor used, the oscillations were assumed to be progressive waves. These waves contained sufficient force to bend the ice and generate the observed water waves (U).

DD FORM 1 JAN 64 1473

UNCLASSIFIED

Security Classification

KEY WORDS	LINK A		LINK B		LINK C	
	ROLE	WT	ROLE	WT	ROLE	WT
Arctic Sea Ice						
Oceanography - Arctic						
Arctic Ocean Surface Waves						
Gravity						
Ice Motion						
Pack Ice						
Pressure, Barometric						
Sea Ice Research						

INSTRUCTIONS

1. ORIGINATING ACTIVITY: Enter the name and address of the contractor, subcontractor, grantee, Department of Defense activity or other organization *(corporate author)* issuing the report.

2a. REPORT SECURITY CLASSIFICATION: Enter the overall security classification of the report. Indicate whether "Restricted Data" is included. Marking is to be in accordance with appropriate security regulations.

2b. GROUP: Automatic downgrading is specified in DoD Directive 5200.10 and Armed Forces Industrial Manual. Enter the group number. Also, when applicable, show that optional markings have been used for Group 3 and Group 4 as authorized.

3. REPORT TITLE: Enter the complete report title in all capital letters. Titles in all cases should be unclassified. If a meaningful title cannot be selected without classification, show title classification in all capitals in parenthesis immediately following the title.

4. DESCRIPTIVE NOTES: If appropriate, enter the type of report, e.g., interim, progress, summary, annual, or final. Give the inclusive dates when a specific reporting period is covered.

5. AUTHOR(S): Enter the name(s) of author(s) as shown on or in the report. Enter last name, first name, middle initial. If military, show rank and branch of service. The name of the principal author is an absolute minimum requirement.

6. REPORT DATE: Enter the date of the report as day, month, year; or month, year. If more than one date appears on the report, use date of publication.

7a. TOTAL NUMBER OF PAGES: The total page count should follow normal pagination procedures, i.e., enter the number of pages containing information.

7b. NUMBER OF REFERENCES: Enter the total number of references cited in the report.

8a. CONTRACT OR GRANT NUMBER: If appropriate, enter the applicable number of the contract or grant under which the report was written.

8b, 8c, & 8d. PROJECT NUMBER: Enter the appropriate military department identification, such as project number, subproject number, system numbers, task number, etc.

9a. ORIGINATOR'S REPORT NUMBER(S): Enter the official report number by which the document will be identified and controlled by the originating activity. This number must be unique to this report.

9b. OTHER REPORT NUMBER(S): If the report has been assigned any other report numbers *(either by the originator or by the sponsor)*, also enter this number(s).

10. AVAILABILITY/LIMITATION NOTICES: Enter any limitations on further dissemination of the report, other than those imposed by security classification, using standard statements such as:

(1) "Qualified requesters may obtain copies of this report from DDC."

(2) "Foreign announcement and dissemination of this report by DDC is not authorized."

(3) "U. S. Government agencies may obtain copies of this report directly from DDC. Other qualified DDC users shall request through _____."

(4) "U. S. military agencies may obtain copies of this report directly from DDC. Other qualified users shall request through _____."

(5) "All distribution of this report is controlled. Qualified DDC users shall request through _____."

If the report has been furnished to the Office of Technical Services, Department of Commerce, for sale to the public, indicate this fact and enter the price, if known.

11. SUPPLEMENTARY NOTES: Use for additional explanatory notes.

12. SPONSORING MILITARY ACTIVITY: Enter the name of the departmental project office or laboratory sponsoring *(paying for)* the research and development. Include address.

13. ABSTRACT: Enter an abstract giving a brief and factual summary of the document indicative of the report, even though it may also appear elsewhere in the body of the technical report. If additional space is required, a continuation sheet shall be attached.

It is highly desirable that the abstract of classified reports be unclassified. Each paragraph of the abstract shall end with an indication of the military security classification of the information in the paragraph, represented as *(TS), (S), (C), or (U)*

There is no limitation on the length of the abstract. However, the suggested length is from 150 to 225 words.

14. KEY WORDS: Key words are technically meaningful terms or short phrases that characterize a report and may be used as index entries for cataloging the report. Key words must be selected so that no security classification is required. Identifiers, such as equipment model designation, trade name, military project code name, geographic location, may be used as key words but will be followed by an indication of technical context. The assignment of links, roles, and weights is optional.

U.S. Naval Oceanographic Office
ON THE GENERATION AND DIRECTIONAL RECORDING OF WAVES IN THE ARCTIC OCEAN, by Leonard A. LeSchack, Sept.1965. 44 p., including 25 figs. (TR-179)

Describes experimental design and results in determination of directionality and generation mechanisms of surface wave action occurring in Arctic Ocean ice. The experiment was conducted at the ONR sponsored drifting station ARLIS II in the vicinity, 73°15'N,157°W. Samples of simultaneous microbarograph and gravimeter recordings are included.

1. Arctic Sea Ice
2. Oceanography - Arctic
3. Arctic Ocean Surface Waves
4. Gravity

i. title: On The Generation and Directional Recording of Waves in the Arctic Ocean
ii. author: Leonard A. LeSchack
iii. TR-179

U.S. Naval Oceanographic Office
ON THE GENERATION AND DIRECTIONAL RECORDING OF WAVES IN THE ARCTIC OCEAN, by Leonard A. LeSchack, Sept.1965. 44 p., including 25 figs. (TR-179)

Describes experimental design and results in determination of directionality and generation mechanisms of surface wave action occurring in Arctic Ocean ice. The experiment was conducted at the ONR sponsored drifting station ARLIS II in the vicinity, 73°15'N,157°W. Samples of simultaneous microbarograph and gravimeter recordings are included.

1. Arctic Sea Ice
2. Oceanography - Arctic
3. Arctic Ocean Surface Waves
4. Gravity

i. title: On The Generation and Directional Recording of Waves in the Arctic Ocean
ii. author: Leonard A. LeSchack
iii. TR-179

U.S. Naval Oceanographic Office
ON THE GENERATION AND DIRECTIONAL RECORDING OF WAVES IN THE ARCTIC OCEAN, by Leonard A. LeSchack, Sept.1965. 44 p., including 25 figs. (TR-179)

Describes experimental design and results in determination of directionality and generation mechanisms of surface wave action occurring in Arctic Ocean ice. The experiment was conducted at the ONR sponsored drifting station ARLIS II in the vicinity, 73°15'N,157°W. Samples of simultaneous microbarograph and gravimeter recordings are included.

1. Arctic Sea Ice
2. Oceanography - Arctic
3. Arctic Ocean Surface Waves
4. Gravity

i. title: On The Generation and Directional Recording of Waves in the Arctic Ocean
ii. author: Leonard A. LeSchack
iii. TR-179

U.S. Naval Oceanographic Office
ON THE GENERATION AND DIRECTIONAL RECORDING OF WAVES IN THE ARCTIC OCEAN, by Leonard A. LeSchack, Sept.1965. 44 p., including 25 figs. (TR-179)

Describes experimental design and results in determination of directionality and generation mechanisms of surface wave action occurring in Arctic Ocean ice. The experiment was conducted at the ONR sponsored drifting station ARLIS II in the vicinity, 73°15'N,157°W. Samples of simultaneous microbarograph and gravimeter recordings are included.

1. Arctic Sea Ice
2. Oceanography - Arctic
3. Arctic Ocean Surface Waves
4. Gravity

i. title: On The Generation and Directional Recording of Waves in the Arctic Ocean
ii. author: Leonard A. LeSchack
iii. TR-179

U.S. Naval Oceanographic Office
ON THE GENERATION AND DIRECTIONAL RECORDING OF WAVES IN THE ARCTIC OCEAN, by Leonard A. LeSchack, Sept.1965. 44 p., including 25 figs. (TR-179)

Describes experimental design and results in determination of directionality and generation mechanisms of surface wave action occurring in Arctic Ocean ice. The experiment was conducted at the ONR sponsored drifting station ARLIS II in the vicinity, 73°15'N,157°W. Samples of simultaneous microbarograph and gravimeter recordings are included.

1. Arctic Sea Ice
2. Oceanography - Arctic
3. Arctic Ocean Surface Waves
4. Gravity

i. title: On The Generation and Directional Recording of Waves in the Arctic Ocean

ii. author: Leonard A. LeSchack

iii. TR-179

U.S. Naval Oceanographic Office
ON THE GENERATION AND DIRECTIONAL RECORDING OF WAVES IN THE ARCTIC OCEAN, by Leonard A. LeSchack, Sept.1965. 44 p., including 25 figs. (TR-179)

Describes experimental design and results in determination of directionality and generation mechanisms of surface wave action occurring in Arctic Ocean ice. The experiment was conducted at the ONR sponsored drifting station ARLIS II in the vicinity, 73°15'N,157°W. Samples of simultaneous microbarograph and gravimeter recordings are included.

1. Arctic Sea Ice
2. Oceanography - Arctic
3. Arctic Ocean Surface Waves
4. Gravity

i. title: On The Generation and Directional Recording of Waves in the Arctic Ocean

ii. author: Leonard A. LeSchack

iii. TR-179

U.S. Naval Oceanographic Office
ON THE GENERATION AND DIRECTIONAL RECORDING OF WAVES IN THE ARCTIC OCEAN, by Leonard A. LeSchack, Sept.1965. 44 p., including 25 figs. (TR-179)

Describes experimental design and results in determination of directionality and generation mechanisms of surface wave action occurring in Arctic Ocean ice. The experiment was conducted at the ONR sponsored drifting station ARLIS II in the vicinity, 73°15'N,157°W. Samples of simultaneous microbarograph and gravimeter recordings are included.

1. Arctic Sea Ice
2. Oceanography - Arctic
3. Arctic Ocean Surface Waves
4. Gravity

i. title: On The Generation and Directional Recording of Waves in the Arctic Ocean

ii. author: Leonard A. LeSchack

iii. TR-179

U.S. Naval Oceanographic Office
ON THE GENERATION AND DIRECTIONAL RECORDING OF WAVES IN THE ARCTIC OCEAN, by Leonard A. LeSchack, Sept.1965. 44 p., including 25 figs. (TR-179)

Describes experimental design and results in determination of directionality and generation mechanisms of surface wave action occurring in Arctic Ocean ice. The experiment was conducted at the ONR sponsored drifting station ARLIS II in the vicinity, 73°15'N,157°W. Samples of simultaneous microbarograph and gravimeter recordings are included.

1. Arctic Sea Ice
2. Oceanography - Arctic
3. Arctic Ocean Surface Waves
4. Gravity

i. title: On The Generation and Directional Recording of Waves in the Arctic Ocean

ii. author: Leonard A. LeSchack

iii. TR-179